



HYBRID LAMINAR FLOW CONTROL (HLFC) RESEARCH AT AIRCRAFT RESEARCH ASSOCIATION (ARA), PAST, PRESENT AND FUTURE

P.W.C. Wong¹, M. Maina² & S. Lawson³

¹IHS Markit ESDU, Ropemaker Place, 25 Ropemaker Street, London, EC2Y 9LY, UK

^{2&3}Aircraft Research Association Ltd, Manton Lane, Bedford, MK41 7PF, UK

Abstract

This paper describes an overview of hybrid laminar flow control (HLFC) research at Aircraft Research Association, current issues and future research recommendations. A transition control methodology for drag reduction has been established in the form of a parametric study for a range of pressure distributions and flow conditions relevant to civil transport aircraft. A single suction chamber with varying porosity concept to alleviate the effect of pressure gradient on the surface suction velocity distribution for delaying transition has been developed. The concept has been integrated into the leading-edge wing structure of a typical civil transport, with the wing ice protection system and high lift system. The resultant structural system is less complex than the multi-chamber concept, and with weight saving. The effect of different types of pressure distributions on transition and aerodynamic performance characteristics for HLFC design has been investigated. A turbulent type of pressure distribution for HLFC design has been applied to a civil transport retrofit wing, as an alternative to a favourable gradient type of pressure distribution. It is shown that transition can be delayed as far downstream as the shock location, and with a higher aerodynamic performance than a favourable gradient type of pressure distribution. The effect of transition region on aerodynamic performance has been shown to be significant and should be included in aerodynamic methods for HLFC wing design. Wind tunnel investigation of transition detection and issues with transition prediction methods and their implications in HLFC design are discussed and future research recommendations are given. Issues with wind tunnel simulation of HLFC wings are discussed and a methodology for simulating full-scale Reynolds number for HLFC wings is described.

Keywords: hybrid laminar flow control, drag reduction, transition, suction system, wind tunnel

Notations

C_D	Drag coefficient.
C_{DF}	Skin friction drag coefficient.
C_{DP}	Pressure drag coefficient.
C_{DV}	Viscous drag coefficient.
C_{DW}	Wave drag coefficient.
C_L	Lift coefficient.
C_p	Pressure coefficient.
d	Hole diameter.
D	Drag.
L	Lift.
M	Mach number.
N	N-factor in stability analysis (amplitude ratio).
p	Pressure

Re	Reynolds number.
\bar{R}	Attachment line Reynolds number.
S_d	Hole spacing to hole diameter ratio.
t	Skin thickness
T	Temperature.
U_∞	Freestream velocity.
V_s	Suction velocity, non-dimensionalised by freestream velocity.
x/c	Streamwise ordinate, non-dimensionalised by chord.
x_e	End transition location.
x_t	Transition location.
α	Angle of incidence.
δ^*	Boundary layer displacement thickness.
ψ	Wave angle.
Λ	Wing sweep angle.

Subscripts

2D	Two-dimensional.
L	Local
n	Normal to wing leading-edge sweep.
w	Wall.
∞	Freestream.

1. Introduction

Drag has a direct impact on aircraft fuel consumption and engine emissions. The increasing emphasis on the environmental effects of engine emissions have driven the need for future civil aircraft to be more environmentally friendly. To this end, there has been large amount of research in recent years into flow control techniques for delaying transition from laminar to turbulent flow in order to reduce drag and fuel burn. One of the techniques that has generated considerable research both in Europe and USA is HLFC. This technology involves the combination of geometry shaping and surface suction in the leading-edge region to control the flow instabilities to delay transition. ARA has carried out HLFC research since the 1980s, and various key findings obtained are described in the paper.

On swept wings, there are number of flow instability mechanisms which can cause transition from laminar to turbulent flow. An important aspect of HLFC is to establish a methodology for controlling these flow instabilities to delay transition. An investigation into a transition control methodology for a range of pressure distributions and flow conditions relevant to civil transport aircraft has been part of the HLFC research programme at ARA since the 1990s [1, 2 & 3]. These research studies have established an appropriate level of suction velocity and suction extent required for controlling various flow instabilities in order to delay transition. The findings are outlined in Section 2 of this paper. In these studies, the surface suction velocity was specified directly in the transition prediction method. Further development of the method has been carried out at ARA to take into account the effect of the pressure difference across the porous surface and surface porosity on the suction mass flow. The method has enabled investigations into the effect of the external pressure gradient and surface porosity on surface suction for a given chamber pressure. The pressure gradient effect is most pronounced in the leading-edge region due to the steep initial flow acceleration. One approach for resolving this problem commonly adopted is the use of a number of separate suction chambers [4], where the suction velocity in each chamber is directly controlled. An alternative approach using a single plenum chamber with varying porosity to alleviate the effect of pressure gradient on the surface suction velocity distribution has been developed at ARA for civil transport and supersonic aircraft [5, 6]. The variable porosity concept for controlling transition is also described in Section 2.

Choosing an appropriate pressure distribution for HLFC wing design is still a key issue at the present time, due to its effect on transition and aerodynamic performance. Aerofoils with different types of

'rooftop' pressure gradients for HLFC application, and their aerodynamic performance characteristics have been investigated at ARA in mid-1990's [7, 8]. Pressure distributions with a favourable 'rooftop' gradient are usually regarded as the most appropriate for maximising laminar flow extent. However, in addition to viscous drag reduction, wave drag and lift capability are important considerations for HLFC wing design. It has been shown that it is possible to obtain a significant extent of laminar flow on aerofoils with an adverse 'rooftop' pressure gradient, that is, the same type of upper surface pressure distribution may be chosen for a HLFC wing as for a turbulent wing. This is also important when considering performance reduction in the event of suction system failure. The choice of an appropriate type of pressure distribution and its design implications, are described in Section 3 of this paper.

The possibility of using a turbulent type of pressure distribution for HLFC design for a civil transport retrofit wing has been investigated at ARA, as an alternative to a favourable gradient type of pressure distribution. It was shown that transition can be delayed as far downstream as the shock location, and with a higher aerodynamic performance than a favourable gradient type of pressure distribution. This conceptual wing design with the single chamber and variable porosity suction system for controlling transition has been integrated with the leading-edge wing structure, combined with the wing ice protection and high lift systems [9]. The resulted suction system in terms of structural complexity and weight relative to a multi-chamber approach is also outlined in Section 4, together with recommendations for its future development.

HLFC analysis tends to focus on transition onset, but the transition process encompasses an intermittency region before the flow becomes fully turbulent. The influence of the transition region on the flow and the effect on the aerodynamic performance of HLFC aerofoils have been shown to be significant in an investigation carried out at ARA [10]. The results suggested that the modelling of the transition region should be included in aerodynamic methods for designing HLFC aerofoils and wings. The effect of transition zone region on aerodynamics performance is described in Section 5 of this paper.

ARA has been involved in Natural Laminar Flow (NLF) and HLFC wind tunnel experimental research since 2000 [11, 12, & 13], and has gained valuable knowledge and experience in transition location measurement techniques and data analysis. Linear stability analysis and the N-factor method is commonly used for transition prediction for HLFC wing design in an industrial environment. The N-factor for transition depends on the flow environment, such as noise and turbulence level. Various issues involving the use of the method for determining a N-factor value for transition for a wind tunnel are discussed in Section 6. For practical NLF and HLFC commercial aircraft wing design, the structural integration of the high lift devices, anti-icing systems and more regular in-service maintenance requirements, may result in a wing with small grooves or steps between these components. A wind tunnel investigation into the effect of various groove and step sizes on transition due to T-S instabilities in NLF, has been carried out at ARA in 2017 [12]. Section 6 also provides outline of this experiment and recommendations for future research.

Wind tunnel testing of aircraft designed for fully turbulent flow in a cryogenic tunnel or in a low Reynolds number facility such as the ARA Transonic Wind Tunnel (TWT) is well established. For aircraft that employ HLFC, the simulation problem is much more complex, and there are testing issues for both types of wind tunnel facilities. A theoretical study to address a number of issues involved in the wind tunnel testing of HLFC wings in a low Reynolds number tunnel and some of the problems related to scale effects has been carried out at ARA in 2000 [14]. The issues with wind tunnel testing methodology of HLFC wing designs and future research recommendations are discussed in Section 7 of this paper.

2. Transition Control Methodology

On swept wings, transition from laminar to turbulent flow may be caused by one of three principal mechanisms which depend mainly on streamwise pressure gradient, Reynolds number and sweep angle. These three mechanisms are attachment line contamination, crossflow (CF) instability and Tollmien-Schlichting (TS) instability. In HLFC, these instability modes can be controlled by means of a combination of surface suction and appropriate streamwise pressure distributions in order to maintain laminar flow. For structural reasons it may be possible to apply suction only on the wing

upper surface upstream of the front spar from about 15% to 20% chord. The control of various instability modes has been investigated in the form of a parametric study at ARA [1, 2]. A range of pressure distributions has been constructed systematically for the parametric studies as illustrated in Figure 1. The pressure distributions consist of a range of initial gradients downstream of the attachment line followed by a range of 'rooftop' gradients. The initial pressure gradient is related to the size of the leading-edge geometry of a section, with a steeper gradient being associated with a smaller leading-edge radius. The range of initial gradients considered in the investigation encompasses both conventional civil transport wings and the Pfenninger-type wing section with its small leading-edge radius and undercut lower surface (see Figure 2).

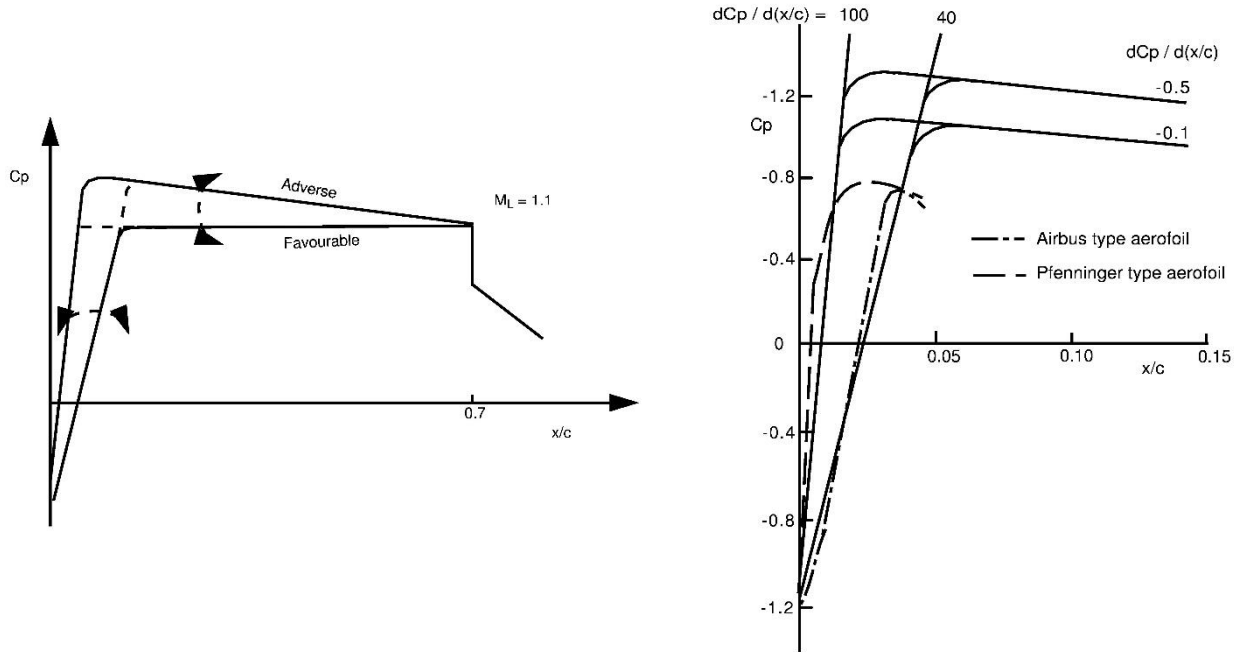


Figure 1 – Sketch of pressure gradient variation Figure 2 – Range of initial pressure distribution

For swept wings, the occurrence of attachment line transition and CF instability is associated mainly with the initial pressure gradient, though favourable 'rooftop' gradients will allow CF instability to persist. TS instability generally becomes dominant further aft, particularly for adverse gradients. Given that these instability modes can be confined to different regions of the wing, a control methodology of treating each mode separately and successively can be employed in HLFC. This is consistent with the use of linear stability analysis for transition prediction, which also presupposes that the instability modes may be treated independently. Linear stability analysis methods coupled with the 'e^N' criterion are widely used for transition prediction. The theory behind such methods has been well documented elsewhere, see for example [15]. The method employed for the work described here is the spatial method, CoDS, due to Atkin [16]. The boundary layer information required as input to CoDS for transition prediction is given by a laminar boundary layer code, BL2D [17, 18]. The integration strategy chosen for the calculation of the N-factor is the constant spanwise wavenumber strategy, which is considered the most physically meaningful for infinite yawed wing flows.

2.1 Attachment Line Contamination

The stability of the attachment line can be assessed based on the magnitude of the attachment line Reynold number, \bar{R} , based on the results of Poll and Paisley [19]. The value of \bar{R} is dependent on the initial pressure gradient, leading-edge sweep and flow condition. For \bar{R} above a critical value of 245, any bursts or spots of turbulence are self-sustaining and will propagate along the attachment line. The gross contamination of the wing by the turbulence originating from the fuselage can be controlled by surface suction or devices such as a 'Gaster bump'. The attachment line boundary layer is also susceptible to TS disturbances. These waves first appear when \bar{R} reaches a value of approximately 580. If \bar{R} exceeds 580 then the waves amplify as they travel along the attachment line and ultimately reach some threshold condition beyond which the waves break down to form localised turbulent spots.

If the local values of \bar{R} drop below 580 then the waves will be damped and eventually die out. For the range of pressure distributions constructed for the parametric study and flow conditions relevant to civil transport, the value of \bar{R} is between 245 and 480, as shown in Figures 3 and 4. This indicates that the stability of the attachment line can be controlled by surface suction or passive devices such as a 'Gaster bump'.

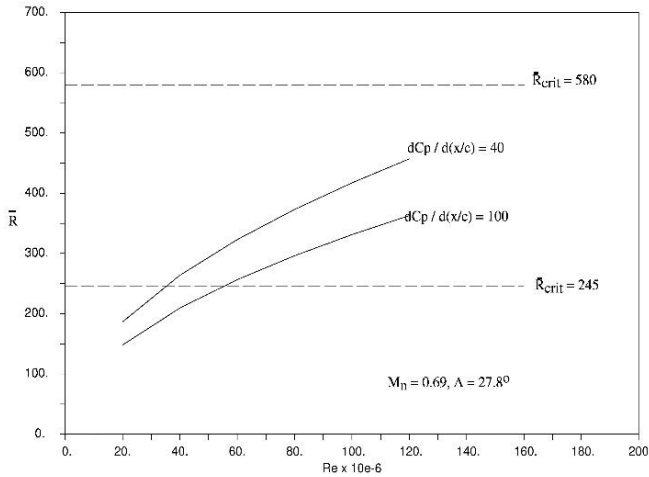


Figure 3 – Effect of initial pressure gradient on \bar{R}

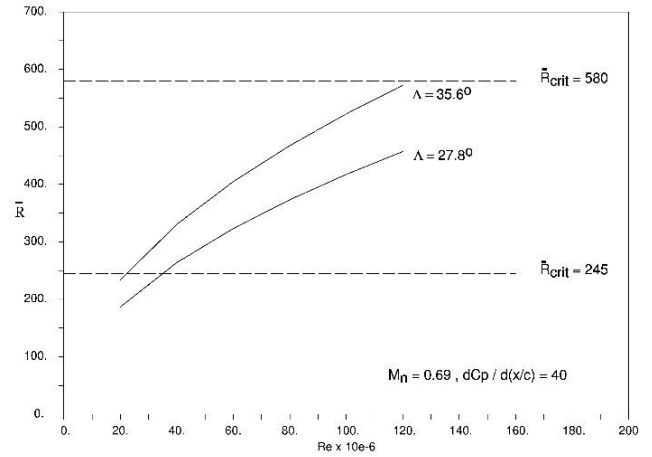


Figure 4 – Effect of sweep angle on \bar{R}

2.2 Crossflow Instability

CF instabilities are due to the inflection point in the crossflow mean velocity profile. These instabilities are strongly dependent on wing leading-edge sweep and the initial flow acceleration corresponding to a favourable pressure gradient. To suppress CF instability, suction is applied over the initial steep pressure gradient region. The required suction velocity is sensitive to pressure gradient and wing sweep as shown in Figures 5 and 6. The results show that although the level of suction required varies with Reynolds number, it tends to become asymptotic and less dependent on the initial pressure gradient and wing sweep. This is beneficial for design in terms of determining a maximum required suction velocity. The maximum level of suction velocity required is about -0.007 for a wing leading-edge sweep of 27.8° for a range of initial pressure gradients. For a wing leading-edge sweep of 35.6° with a low initial pressure gradient of 40, which may be associated with a cruise Mach number of 0.85 for an inboard wing section with a larger leading-edge radius, the maximum suction velocity required is about -0.009. The results have provided useful guidance in the maximum level of suction velocity required for controlling CF in HLFC wing design.

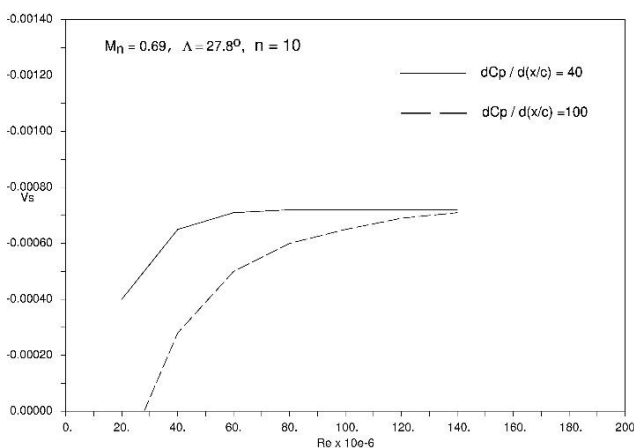


Figure 5 – Effect of initial pressure gradient on suction velocity

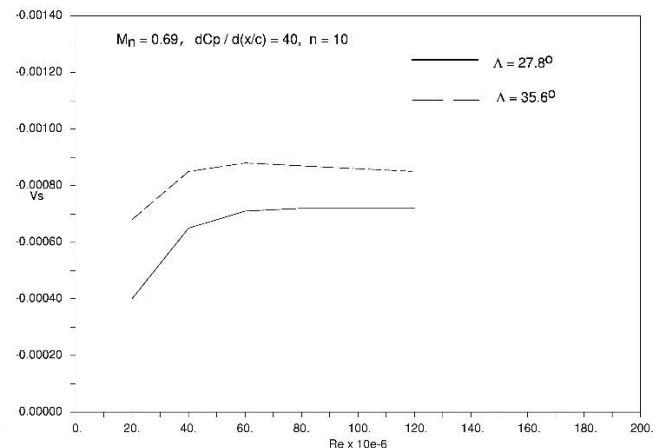


Figure 6 – Effect of sweep on suction velocity

2.3 Tollmien-Schlichting Instability

With the assumption that CF instability has been controlled and the onset of transition delayed to aft of the minimum pressure point, then TS instability would become the dominant mode for transition. Investigations carried out at ARA [3] have shown that the level of suction required for suppressing TS instability is much less than for CF. For most cases a suction velocity of about -0.0002 would be

sufficient for a range of rooftop pressure gradients. It was also found that it is more effective to increase the suction panel length than the suction velocity in order to delay transition, as shown in Figure 7. This implies the structural constraint of the suction panel forward of the front spar may limit the extent of laminar flow which could be achievable. This constraint may be overcome by the use of surface cooling instead of suction downstream of the front spar for suppressing TS instability. The cooling rates required were found to be low, generally about 10% below the ambient temperature is sufficient to delay transition significantly. A transition control methodology consisting of a successive number of suction panels forward of the front spar for suppressing the CF and TS instabilities, combined with cooling panels downstream of the front spar if further extent of laminar flow is required, as illustrated in Figure 8, could be employed.

There is current interest in the use of hydrogen fuel for engine propulsion for zero carbon emissions. One specific challenge is how to store hydrogen on board the aircraft. Today, liquid hydrogen storage is among the most promising options, while storing hydrogen as compressed gas poses challenges with current aircraft weight and volume requirements. Liquid hydrogen is stored in very low temperatures, of the order of -250°C . The feasibility of using the liquid hydrogen to provide surface cooling to suppress the flow instabilities for delaying transition should be investigated in the future.

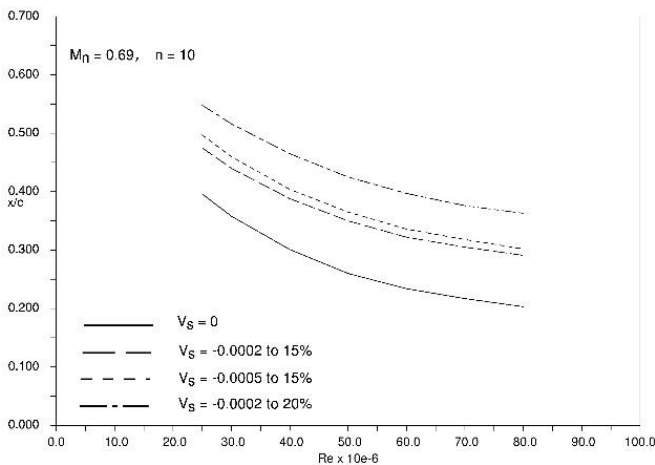


Figure 7 – Effect of initial pressure gradient on suction velocity

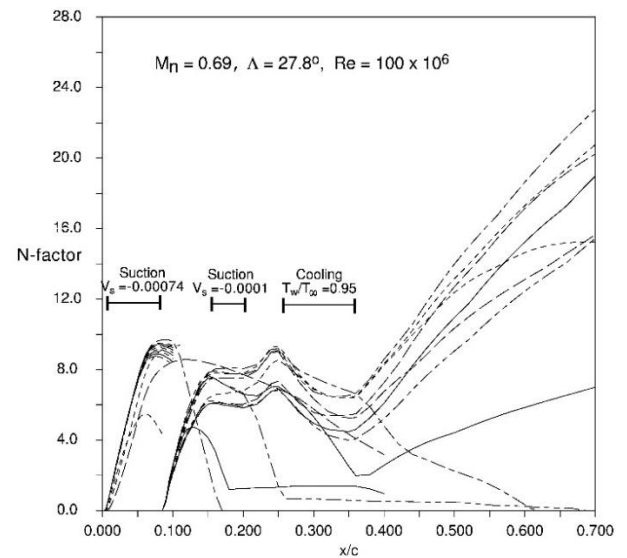


Figure 8 – Illustration of control methodology

2.4 Single Suction Chamber and Variable Porosity Technique

In the parametric studies described in sections 2.2 and 2.3, the surface suction velocity was specified directly in the transition prediction method, the effect of the external pressure gradient on the surface suction velocity has not been taken into account. This effect is most pronounced in the leading-edge region due to the steep pressure gradient associated with the initial flow acceleration. The laminar boundary layer code, BL2D [17, 18], has been modified at ARA to allow the plenum chamber pressure and panel porosity to be specified as input data, rather than the suction velocity. The suction velocity is calculated by an empirical correlation based on the pressure difference across the porous skin [20]. For a constant chamber pressure, the external pressure gradient shown in Figure 2 can cause a large variation in the pressure difference (Δp) across the porous panel and hence the suction velocity distribution (V_s), as illustrated in Figures 9 and 10.

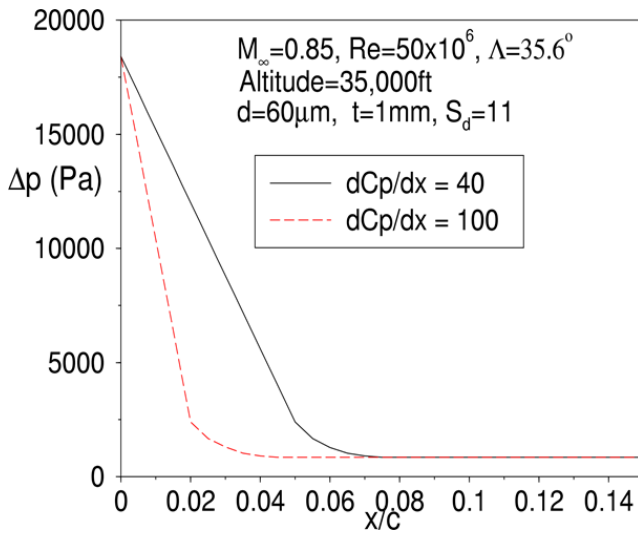


Figure 9 – Pressure difference variation

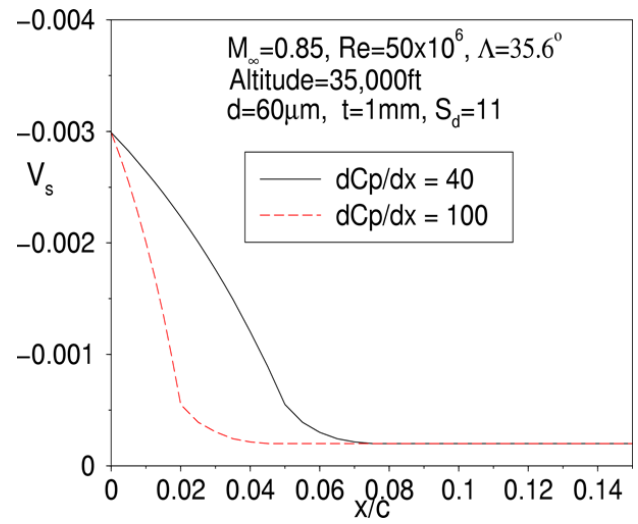


Figure 10 – Suction velocity variation

One approach to resolving this problem is the use of a number of separate suction chambers within a double sheet suction surface [4], where the suction velocity in each chamber is controlled by orifices in the inner sheet and a constant speed suction pump directly coupled with the leading-edge box. To minimize the number of plenum chambers in order to reduce system complexity, ARA has developed an alternative approach to vary the suction panel porosity to balance the effect of pressure gradient [5]. A parameter that affects the panel porosity is the ratio of hole spacing to hole diameter (S_d), where a higher value would give a lower suction velocity. In order to provide a uniform suction velocity across the region with an initial steep pressure gradient, a higher initial value of S_d can be applied at the leading-edge with the value reduced linearly with distance, as shown in Figure 11. It can be seen that the suction velocity distributions in Figure 12 given by the porosity variation are now much more uniform across the initial pressure gradient region. The level of the suction velocity can be further controlled by the hole diameter and/or skin thickness.

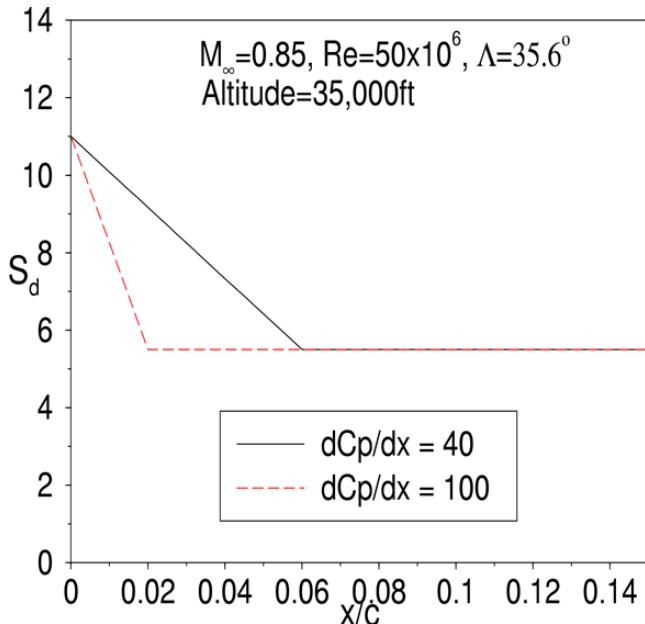


Figure 11 – Porosity variation

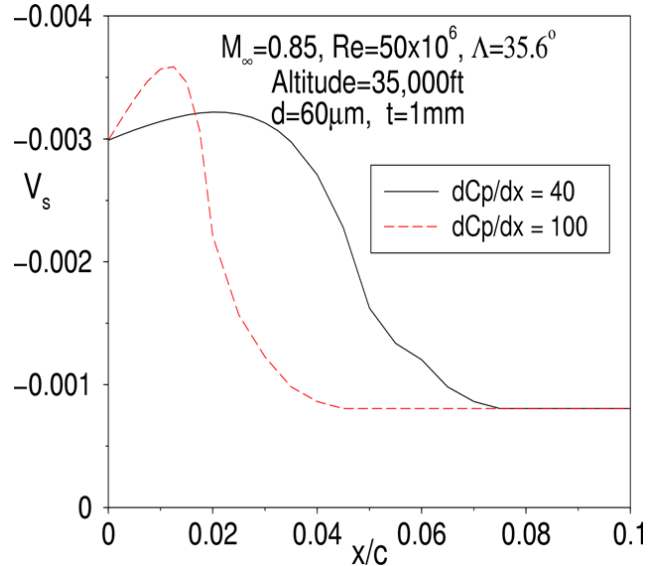


Figure 12 – Suction velocity variation

The single plenum chamber with varying porosity approach to control the suction velocity distribution has also been shown to be applicable to supersonic aircraft [6] in an EU funded project called HISAC (**HIGH SPEED AIRCRAFT**). The HISAC generic baseline configuration which was used for the transition control study is shown in Figure 13. A significant extent of laminar flow can be achieved using the variable porosity technique, with a drag reduction (ΔC_{DV}) of 28.5% for $C_L=0.1$ and 11.7% for $C_L=0.175$ at the cruise Mach number $M=1.6$, as shown in Figure 14.

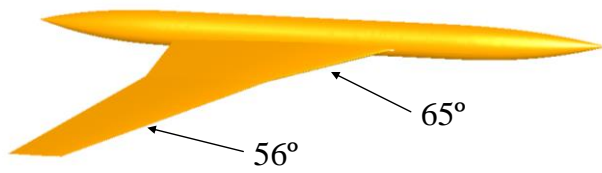


Figure 13 – HISAC baseline geometry

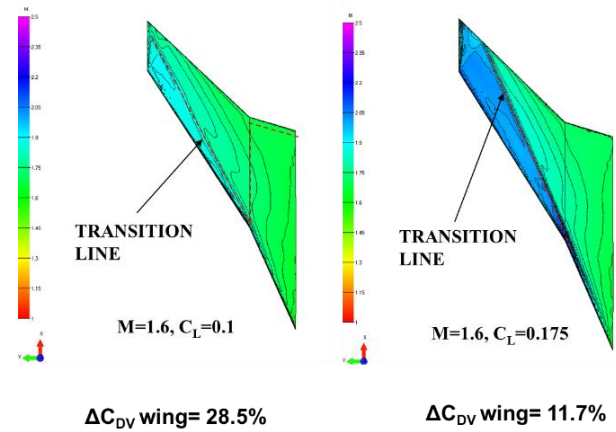


Figure 14 – Surface Mach number distributions and transition locations with surface suction applied

The porosity variation for controlling the suction velocity due to the effect of the pressure gradient in the initial accelerated flow leading-edge region is illustrated in Figure 15, where S_d is reduced linearly with distance by a factor of a half from 0 to 1% chord and then increased linearly by a factor of a half from 1% to 20% chord. The effect of this variation in porosity on the surface suction velocity distribution, assuming the same chamber pressure, is also shown in Figure 15. The benefit of variable porosity compared with constant porosity on the N-factor distribution for transition can be seen in Figure 16, where a significant extent of laminar flow to 65% chord for the inboard wing has been achieved with variable porosity if transition onset is assumed to occur at N-factor of 10.

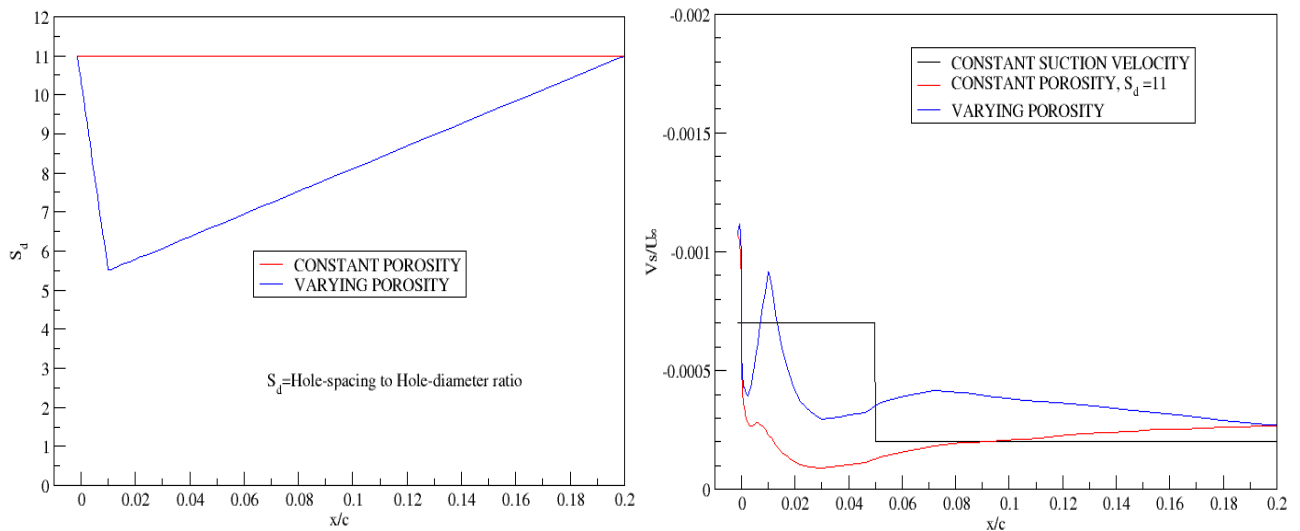


Figure 15 – Porosity distributions and suction velocity variation

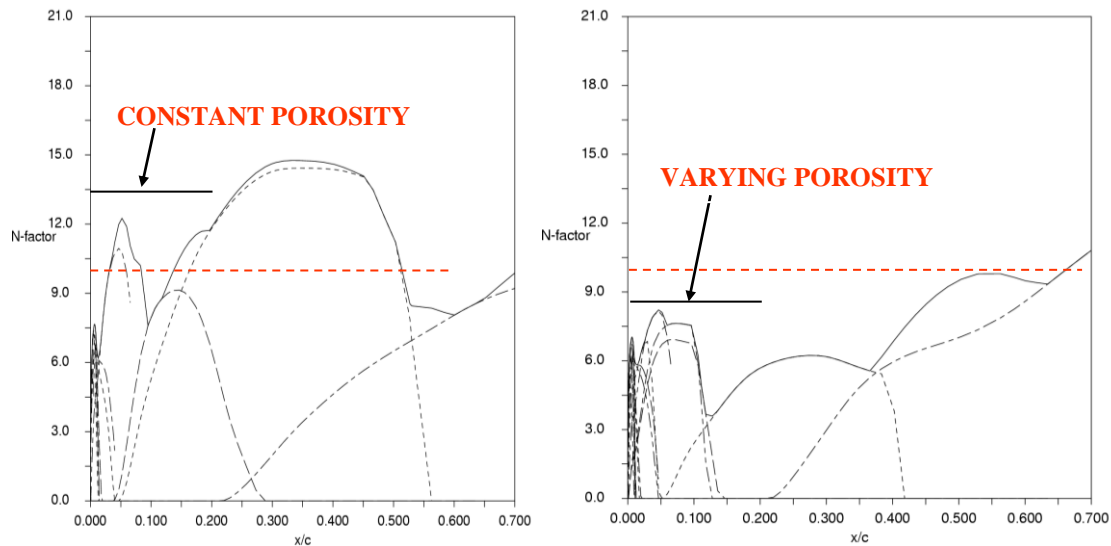


Figure 16 – Effect of porosity distribution on the N-factor distributions
Inboard wing, $M=1.6$, $C_L=0.1$, $Re=75.3 \times 10^6$

3. Choice of Pressure Distributions

It is difficult to choose an appropriate 'rooftop' pressure distribution for optimum aerodynamic performance in HLFC wing design. For maximizing the laminar flow extent, pressure distributions with a favourable 'rooftop' gradient are usually regarded as the most appropriate. However, in addition to viscous drag reduction, wave drag and lift capability are important considerations for HLFC wing design. ARA has been investigating these design issues since 1990s [1, 2 & 9]. The design issues can be illustrated by an analysis of the aerodynamic performance characteristics of two aerofoils with pressure distributions which may be suitable for HLFC application, one with a favourable 'rooftop' pressure gradient and the other with an adverse pressure gradient. Both aerofoils have an 'rooftop' extent of 60-70% chord in the design condition, as shown in Figures 17 and 18. A suction velocity of -0.0007 from 0 to 5% chord and -0.0002 from 5% to 15% chord has been applied for suppressing CF and TS instabilities respectively to allow a significant extent of laminar flow. The drag characteristics and performance characteristics in terms of ML/D for the aerofoils are compared in Figures 19 and 20, respectively. As illustrated in the results, despite the transition position on the favourable pressure gradient aerofoil being further aft than on the adverse pressure gradient aerofoil, the adverse gradient aerofoil has a higher lift capability for a given shock strength and better drag rise characteristics than the favourable gradient aerofoil. This implies that the same type of upper surface pressure distribution can be chosen for a hybrid laminar flow wing as for a turbulent wing. This is also important for ensuring a viable wing design in terms of performance in the event of suction failure.

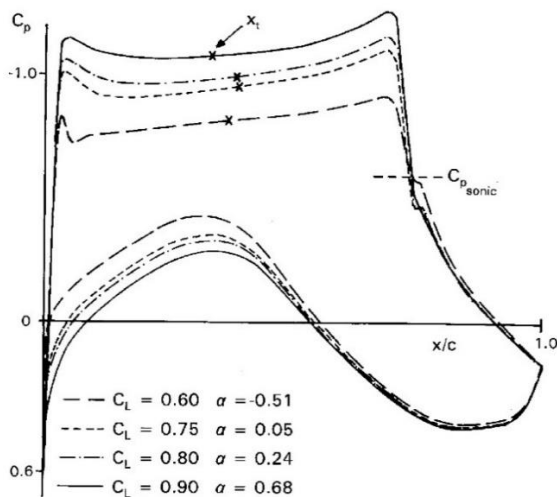


Figure 17 – Favourable pressure gradient aerofoil, $M=0.75$, $Re=35 \times 10^6$

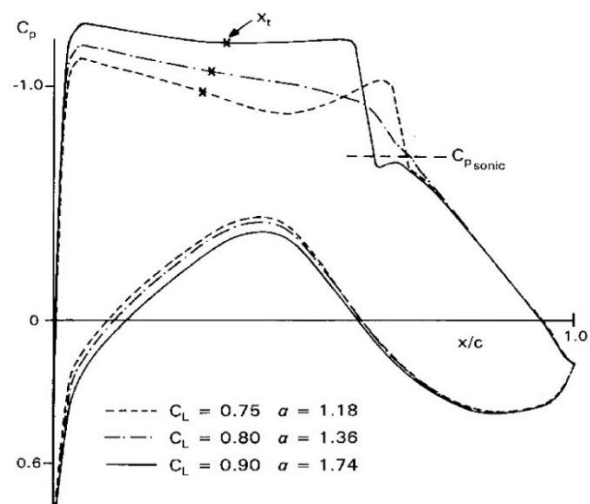


Figure 18 – Adverse pressure gradient aerofoil, $M=0.75$, $Re=35 \times 10^6$

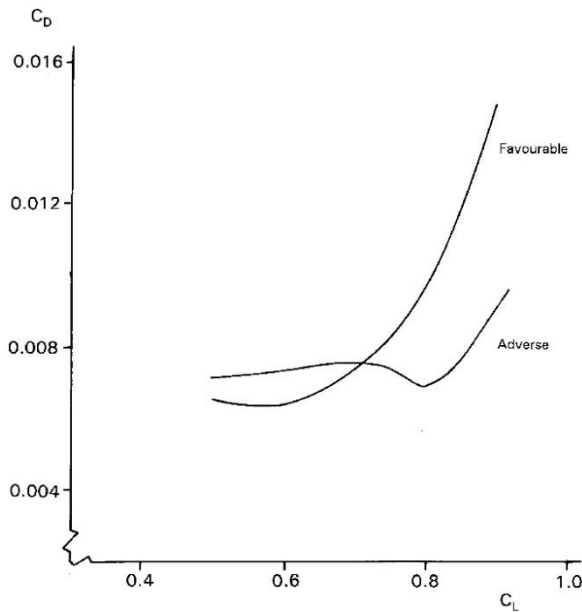


Figure 19 – Drag characteristics

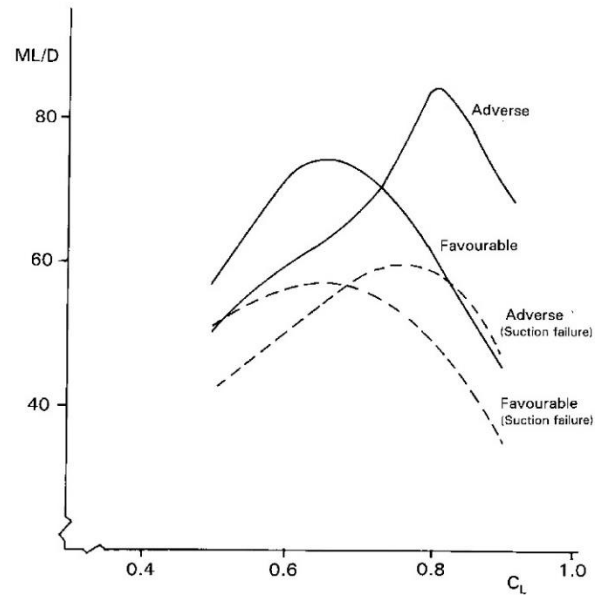


Figure 20 – Performance characteristics

4. Suction System and Structural Integration

4.1 Variable Porosity Technique

The single suction chamber and variable porosity technique with a turbulent type of pressure distribution for HLFC design, has been applied to an Airbus A330 aircraft outer wing retrofit, under an EU funded research programme called AFLONEXT (**A**ctive **F**low, **L**oad & **N**oise **C**ontrol on **n**ext generation aircraft). Various degrees of pressure gradient for the upper surface and their effect on transition control and aerodynamic performance have been investigated [9]. The design constraints were to maintain the maximum thickness/chord ratio and aft part of the geometric profile same as the baseline section. The pressure distributions for three of the sections that have been derived based on the baseline geometry in the design investigation are shown in Figure 21. It can be seen from Figure 22, for a given design C_L , the lift to drag ratio, L/D , for Designs B and C with a turbulent type of pressure distribution are higher than Design A with a favourable gradient type of pressure distribution. The turbulent designs also have a weaker shock and lower drag rise than the design with a favourable type of pressure gradient, as shown in Figures 21 and 23, respectively.

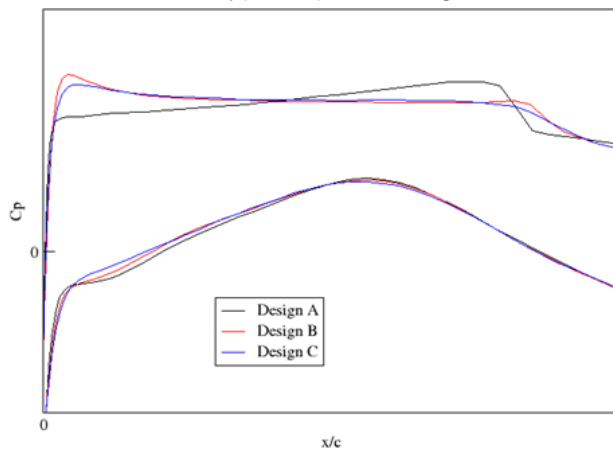
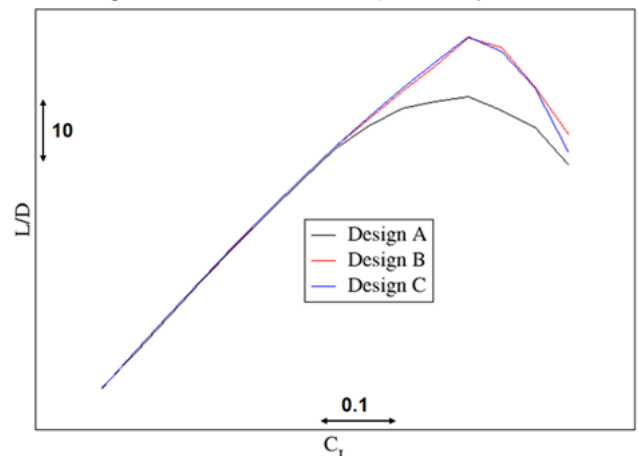


Figure 21 – 2D pressure distributions, $M=0.75$,
 $M_{2D}=0.708$, $C_L=0.76$, $Re=19.81 \times 10^6$

Figure 22 – L/D performance

For the designs with a turbulent type of pressure distribution, it is possible to use a single suction chamber with variable porosity to delay transition as far downstream as the shock location. For the pressure distributions shown in Figure 21, the steep pressure gradient occurs close to the leading-edge, within the initial 2% chord, and its variation with distance over this region is nearly linear. Based on the transition control methodology established in [5, 6] outlined in Section 2.4, a higher value of s/d can be applied at the leading-edge and then reduced linearly with distance. The variation of

porosity with distance could be defined in various ways, and it was shown that two types of porosity variation as shown in Figure 24 could be used to provide an appropriate suction velocity distribution for controlling transition. One of these cases is a linear reduction in s/d by 50% over the initial 2% chord followed with a constant porosity to 20% chord, defined as ‘two-part’ variable porosity distribution, and the other is simply a linear variation from the leading-edge to 20% chord.

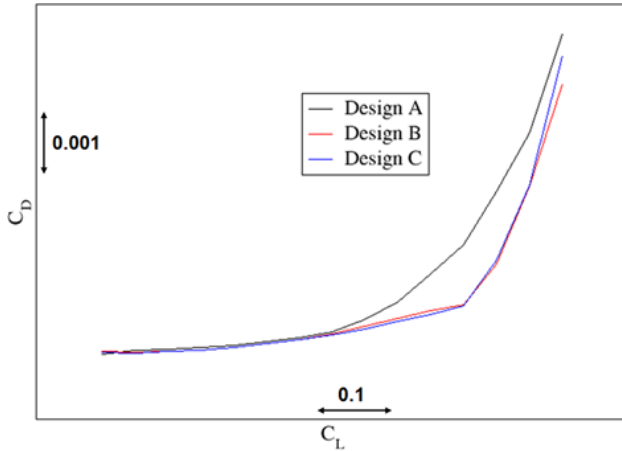
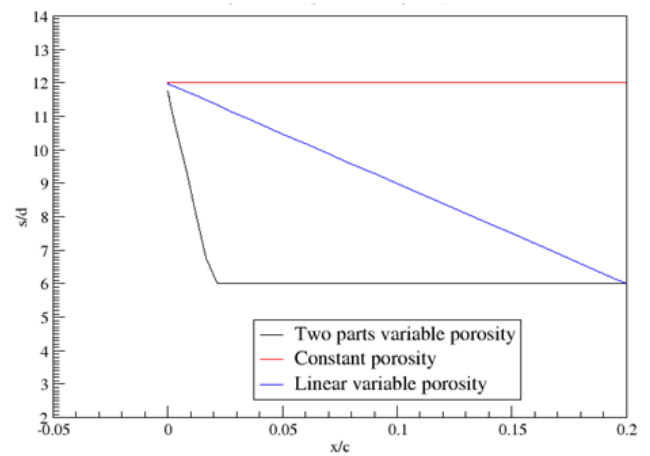
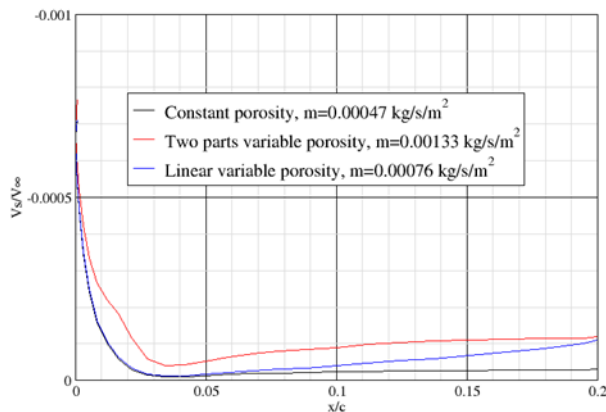
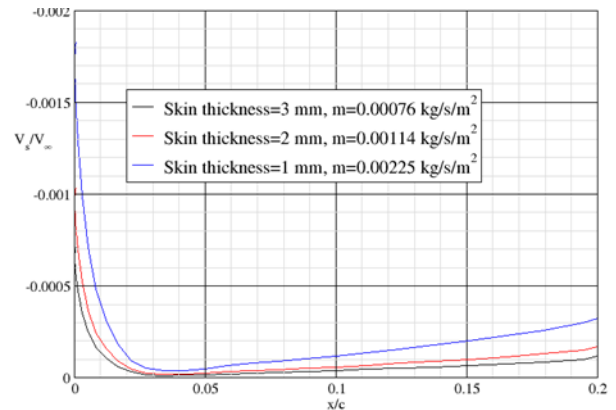


Figure 23 – Drag performance

Figure 24 – Porosity distributions, $d=50\mu\text{m}$

For surface suction, the chamber pressure needs to be lower than the external pressure, otherwise, blowing would occur, which could cause transition. A lower chamber pressure would give a higher suction velocity and mass flow, and requires a higher suction pump power. For the single chamber and variable porosity technique, the suction pump power requirement could be minimized by setting the chamber pressure at a level just low enough to avoid blowing. This chamber pressure is sufficient to provide an appropriate suction velocity across the porous panel for controlling the flow instabilities to delay transition. This is illustrated in Figure 25, with a higher suction velocity in the initial steep pressure gradient region for controlling CF instability and a reduced level downstream of this region for controlling TS instability. The level of suction velocity distribution can be further controlled by a combination of the porosity variation, suction hole diameter and skin thickness, in order to achieve an appropriate level for delaying transition. For example, Figure 26 shows that the level of suction can be increased by reducing the skin thickness. It should be noted that for the constant porosity distribution, it has not been possible to achieve an appropriate level of suction velocity distribution, it is either too high in the initial steep pressure gradient region or too low downstream of this region. The single chamber and variable porosity concept can be easily adapted for different porosity distributions with various hole diameters and skin thicknesses. Future research is required to study the trade-off between the structural stiffness, weight and laser drilling in terms of hole spacing, hole diameter and skin thickness for the porous skin.

Figure 25 – Design C suction velocity distribution, chamber pressure=13250Pa, $d=50\mu\text{m}$, $t=3\text{mm}$ Figure 26 – Effect of skin thickness on suction velocity distribution, Design C, chamber pressure=13250Pa, $d=50\mu\text{m}$

4.2 Structural Integration

The single chamber and variable porosity suction system has been integrated into the leading-edge wing structure of the Airbus A330 aircraft outer wing retrofit, with the wing ice protection system and high lift system [9]. The structural integration was based on the modification of an existing multi-chamber geometry, with most of the structural features maintained. The resultant structural system is less complex than the multi-chamber geometry, and with an appreciable weight saving.

The single chamber consists of an outer porous skin and a solid inner skin with suction holes. The multi-chamber internal structures have been totally removed to create a single chamber, with the depth of the chamber between the outer and inner skin remained the same. The outer skin with constant porosity of the multi-chamber geometry has been replaced with a skin with variable porosity distribution in the chordwise direction. There are three rows of internal ribs in the suction chamber to support the outer skin under load deflection as shown in Figure 27. These ribs are evenly spaced across the span, with cuts to enable air to pass through in the spanwise direction. These ribs could be placed across the span if necessary, instead of in the chordwise direction as currently shown. The inner skin has four rows of suction holes to minimise the spanwise variation in suction as shown in Figure 27. The suction air is passed through these suction holes into the collector ducts underneath the inner skin as shown Figure 28. The collector ducts are connected to two trunk pipes via two collector pipes, one for the suction air supply and the other for the hot air supply for the wing ice protection system.

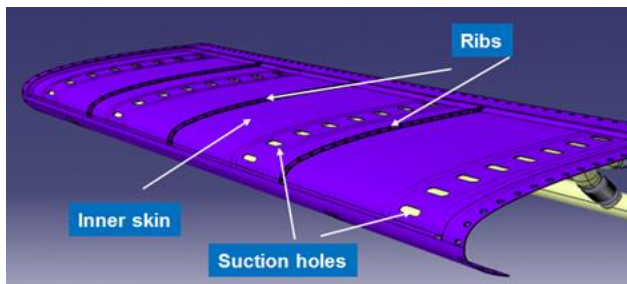


Figure 27 – Inner skin with suction holes and internal ribs

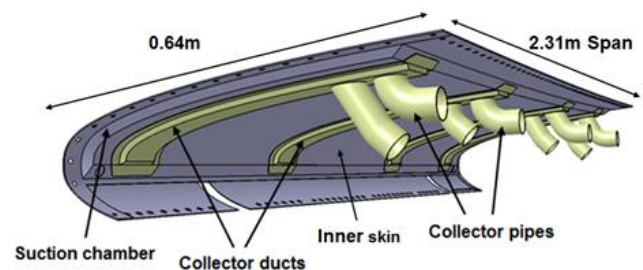


Figure 28 – Collector ducts and collector pipes underneath the inner skin

The weight estimates for the part of the suction skin structural system for the single chamber and

variable porosity concept illustrated in Figure 28 are shown in Table 1. The weight for an equivalent structural system for the multi-chamber concept is also included for comparison. The weight estimation carried out for the HLFC structure as shown in Figure 28 is purely for assessing the relative weight between the two concepts. It can be seen in Table 1 that the weight for single chamber concept is about 44% lighter than the multi-chamber concept with a wing span of 2.31m. For the whole wing structure of an aircraft, the single chamber and variable porosity concept would have a significant weight saving compared with the multi-chamber concept.

Design concepts	Hole diameter (microns)	Weight (kg)
Multi-chamber concept	60	27.62
Single chamber concept	60	15.55
	50	15.54

Table 1 – Comparison of weight estimates

5. Intermittency Region

The analysis so far has been focusing on transition onset, but the influence of the transition region on the flow and the effect on the aerodynamic performance of HLFC aerofoils can be significant as shown in an investigation carried out at ARA [10]. This can be seen in the results presented in Figures 29 to 31 for two aerofoils with different types of upper surface pressure distribution, one with a favourable 'rooftop' pressure gradient (M2303 aerofoil) and the other with an adverse gradient (Lock aerofoil).

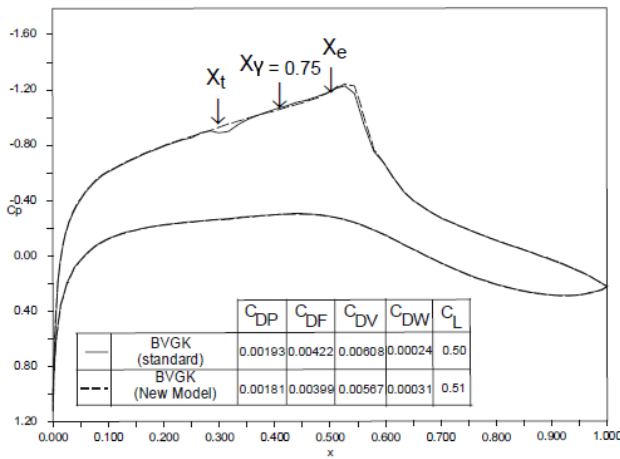


Figure 29 – Effect of transition zone on HLFC aerofoil performance, M2303 aerofoil, $M = 0.68$, $R = 35 \times 10^6$, $\alpha = 2.8^\circ$

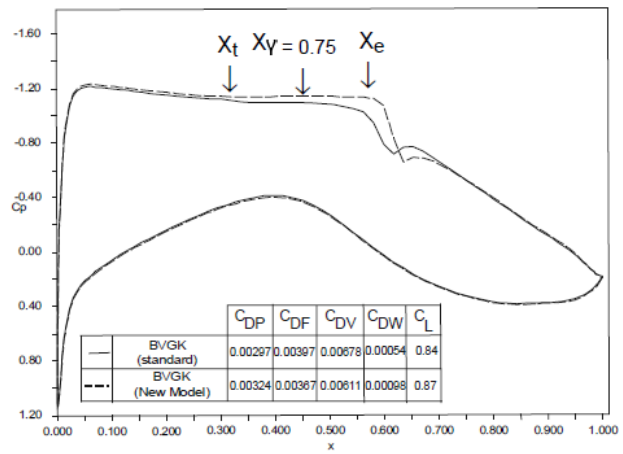


Figure 30 – Effect of transition zone on HLFC aerofoil performance, Lock aerofoil, $M = 0.72$, $R = 35 \times 10^6$, $\alpha = 1.5^\circ$

These results were obtained using an aerofoil computer code BVGK [21], where the ‘standard’ version is with transition fixed at the onset location and the ‘new model’ with a transition zone model based on modification of the boundary layer intermittency model due to Narasimha and Dey [22]. These aerofoils have been assumed to be the two-dimensional sections equivalent to an infinite yawed wing with 35° leading-edge sweep. For these sections, transition onset at a flight Reynolds number of 35×10^6 occurs at about 30% chord, where a suction velocity of -0.0007 from 0 to 5% chord and -0.0002 from 5% to 15% chord has been applied for suppressing the various modes of instability. The predicted transition zone length is about 15% chord and its effect on the pressure distribution is small compared to a transition fixed case at the onset location, but its effect on the aerodynamic performance is significant. The results suggested that the modelling of the transition region should be included in aerodynamic methods for designing HLFC aerofoils and wings.

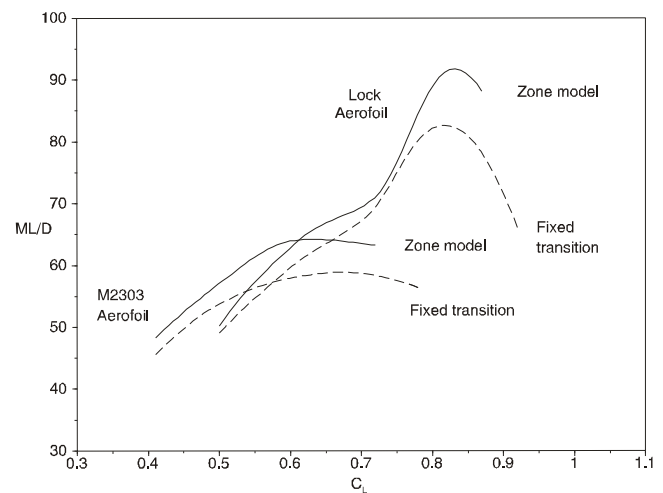


Figure 31 – Effect of transition region on ML/D performance

6. Transition Measurement and Prediction

Several research projects have been carried out over the past years at ARA to develop wind-tunnel test techniques for detecting transition for NLF and HLFC configurations [11, 12, & 13]. The experiment in [11] involved a NLF swept wing panel with the aim of determining a N-factor for transition for the ARA TWT and to validate the linear stability analysis method for transition prediction [16]. The wind tunnel test in [12] measured the effects of small surface irregularities on laminar flow extent. The investigation in [13] involved experimental techniques for a HLFC concept with a single chamber and variable porosity for delaying transition, where transition prediction analysis of the HLFC wind tunnel test data was carried out in [23].

6.1 Wind Tunnel N-Factor for Transition

A swept wing panel with NLF flow design was tested in ARA TWT, within the **Smart Active Wing of the Future**, SAWoF, programme funded by the UK government [11]. The aim of the test was to provide qualification of the flow quality and suitability of ARA TWT for laminar flow testing. Various techniques for detecting transition were used in the experimental investigation (see Figure 32),

including temperature sensitive paint (TSP) and infra-red (IR) thermography for measuring the whole transition process from onset to completion indicated in Figure 33. This is the same model as used in the experiment performed in the DERA wind tunnel in [24].

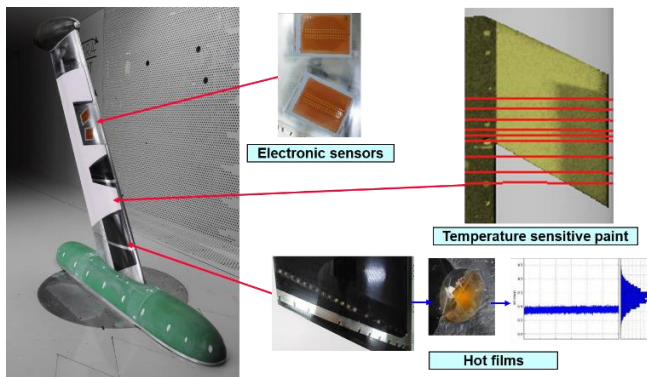


Figure 32 – NLF wind tunnel model and instrumentation, sweep angles 0°, 25° and 30°, Mach numbers between 0.45 and 0.85

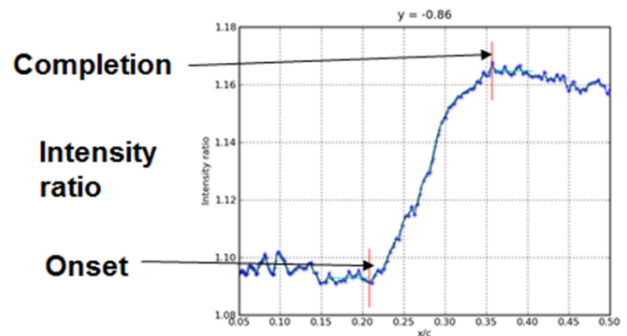


Figure 33 – Temperature sensitive paint for transition measurement

The transition onset locations for a range of wind tunnel conditions have been analysed with the linear stability analysis transition prediction method, CoDS [16]. Linear stability analysis and the 'e^N' method is commonly used in the aerospace industry for transition prediction. With these methods, the onset of transition occurs when the growth of various flow instability modes has reached a certain level governed by the value of N, known as the N-factor.

The flow environment, such as noise and turbulence affect transition location, and the onset of transition is calibrated by the N-factor with the linear stability method. The higher the noise and turbulence level in the flow environment, the lower the N-factor for transition. For flight, the N-factor for transition may be in the range of 15 to 20. In contrast, for wind tunnels, where freestream flow quality is worse than in flight conditions, this value is likely to be in the region of 6 to 10. It was established that the N-factor for transition for ARA TWT is about 7.5 as shown in Figure 34, which is well within the range for similar industrial transonic wind tunnels, indicating that the tunnel is suitable for laminar flow testing.

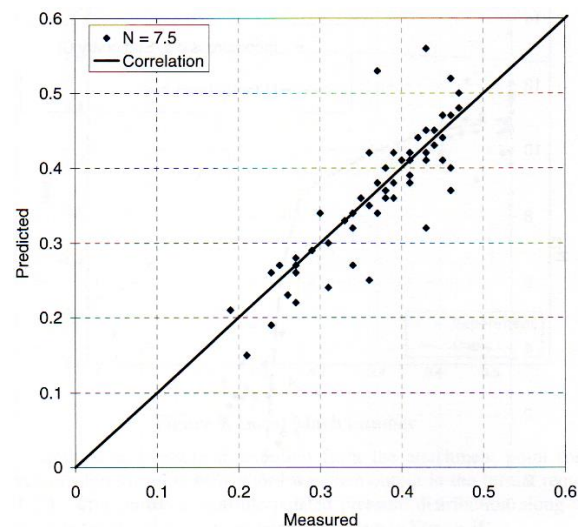


Figure 34 – N-factor for transition of ARA TWT

6.2 Surface Imperfections

Surface imperfections in the wing leading-edge region could result from the structural integration of various components such as the high-lift devices and anti-icing system, where small steps or grooves may occur between these components. The effect of steps and grooves on transition has been investigated in the ARA TWT [12] under the ATI/IUK ALFET (Advanced Laminar Flow Enabling Technologies) programme led by Airbus which aimed to develop the understanding and tools required to design and build a natural laminar flow wing. A ring wing model shown in Figure 35, was designed and manufactured with a NLF aerofoil section and provision to install a variety of surface imperfections. The model was manufactured with a high quality surface finish and fitted with instrumentation to measure laminar flow extent, including an insulating panel for use with IR thermography and hot films as shown in Figure 36.

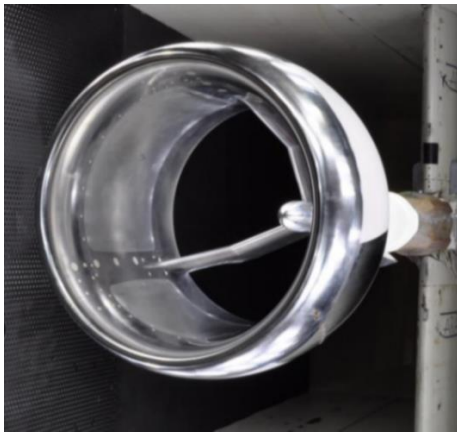


Figure 35 – ALFET Model installed in the ARA TWT

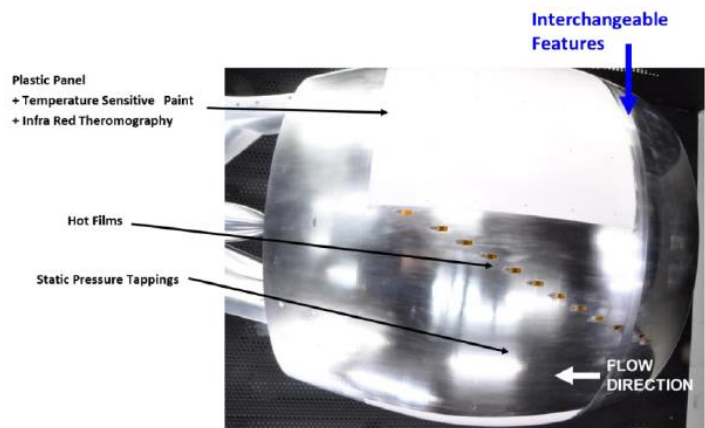


Figure 36 – Side view of the installed measurement system

The model was tested over a range of Mach numbers from $M = 0.574$ to $M = 0.785$ for grooves of different depths, defined by a groove parameter. An example of an IR image showing transition onset locations is illustrated in Figure 37. The location for transition onset and completion were obtained from the intensity ratio distribution from the IR data as shown Figure 37 for a slice at location 5.2.1. A large quantity of transition data for various groove parameters and Mach numbers were obtained. An example test result showing the effect of the groove parameter on transition position is presented in Figure 38. It was found that the groove has the effect of forcing transition forward more strongly at lower than at higher Mach numbers [12]. ARA has acquired the wind tunnel testing capability for measuring the effect of small features on transition in NLF, and the knowledge gained could be extended to HLFC to investigate the effect of suction on the disturbances due to various degrees of surface imperfections in the future.

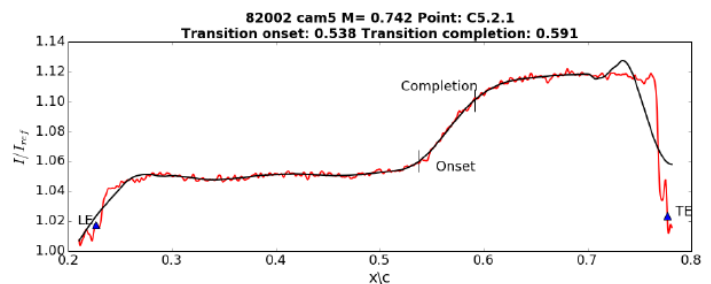
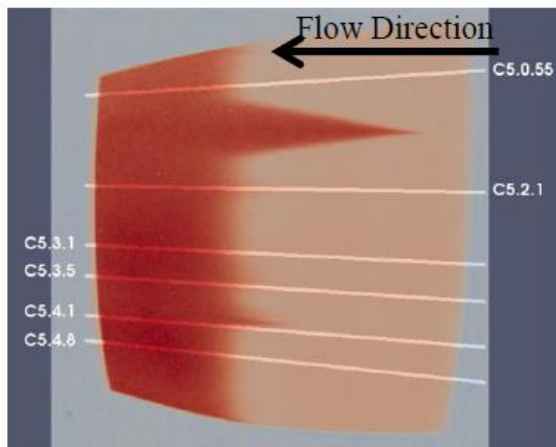


Figure 37 – Infra-red example data

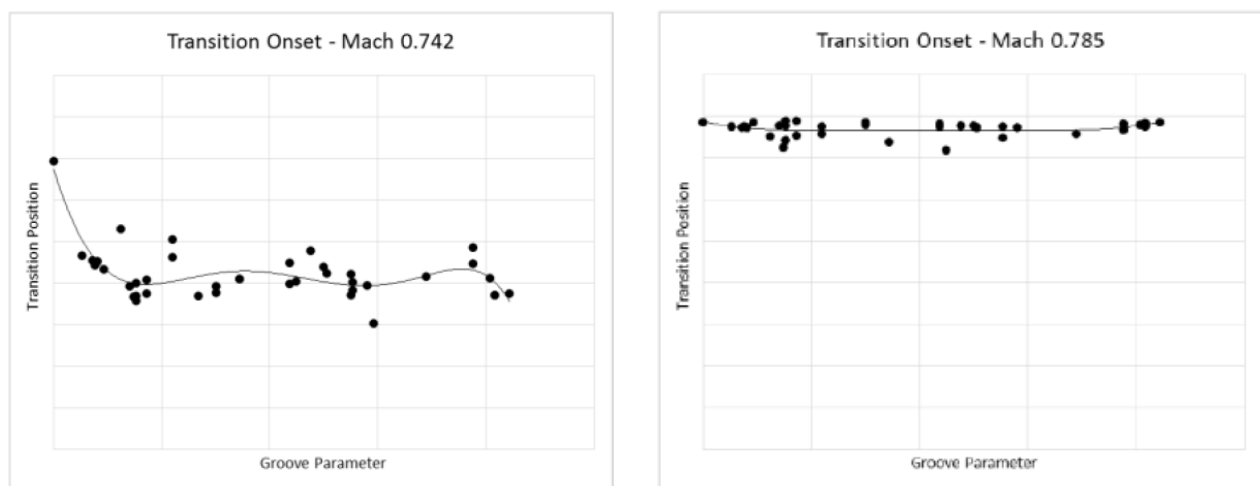


Figure 38 – Effect of the groove parameter on the transition position

6.3 HLFC and Variable Porosity

A HLFC wind tunnel model with a variable porosity surface has been tested in ARA TWT [13]. The HLFC wind tunnel model was specifically designed in a modular form, with the mid-span leading-edge region interchangeable for various porous panels, as shown in Figure 39. The aim of the wind tunnel experiments was to demonstrate, for the types of pressure distribution relevant to civil transport aircraft design, the effectiveness of a range of transition control techniques. Additional test objectives included generating a data set for method validation and to evaluate the suction properties of porous plates. The pressure distribution of the aerofoil section normal to leading-edge sweep of 35° for the design condition at $M=0.85$ is shown in Figure 40. Three different panels were tested, a solid panel, a constant porosity panel and variable porosity panel. The porous panels had $45\ \mu\text{m}$ diameter holes, providing porosity from the leading-edge to 20% chord on the upper surface. The constant porosity panel had a hole spacing to hole diameter ratio (s/d) of 12, while the variable porosity panel had a linear variation of s/d from 12 at the leading-edge to 8 at 5% chord returning back to 12 at 20% chord, as shown in Figure 41. Wind tunnel tests using the HLFC model are described in [13] and the analysis of the results using local linear stability [16] and linear parabolised stability equations analysis [25, 26] is given in [23]. This work was undertaken as part of the ARCADE programme, a research project funded by the UK Department of Business, Energy & Industrial Strategy (BEIS) and Innovate UK (IUK).

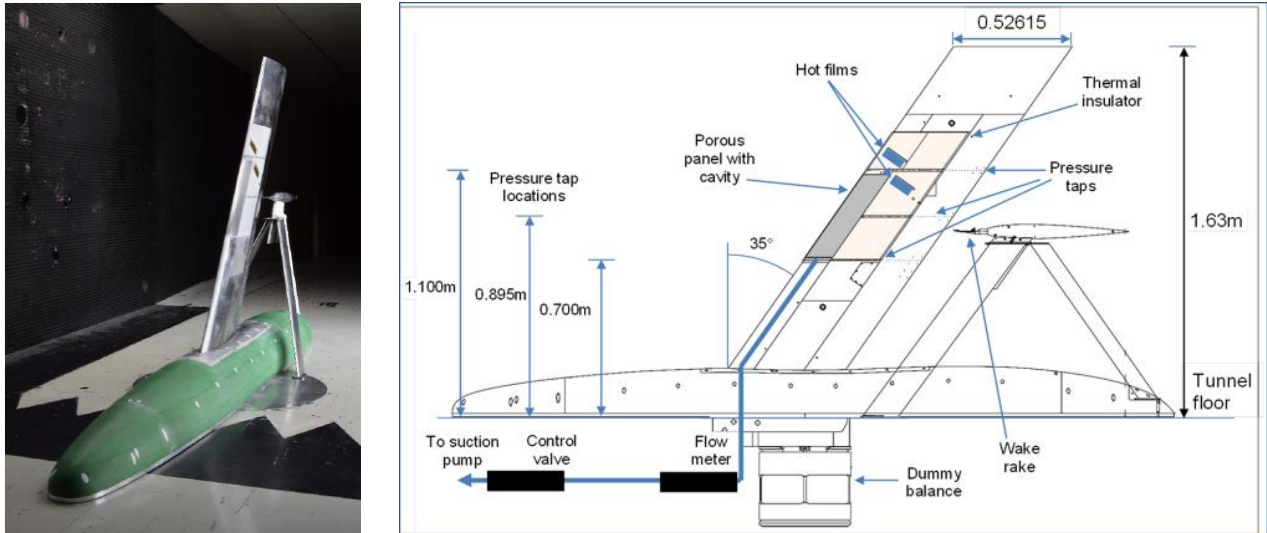


Figure 39 – HLFC wind tunnel model

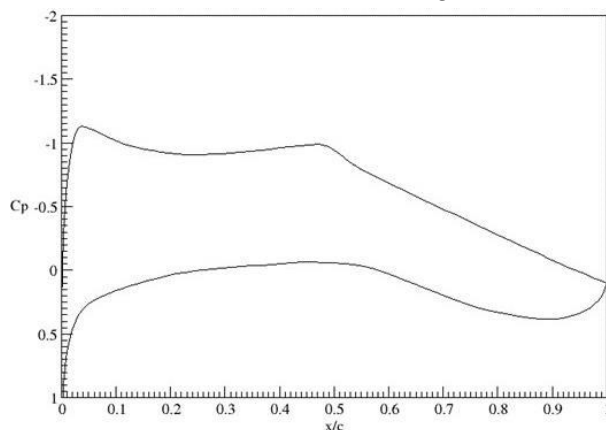


Figure 40 – Two-dimensional pressure distribution, $M=0.85$, $\alpha=1.8^\circ$

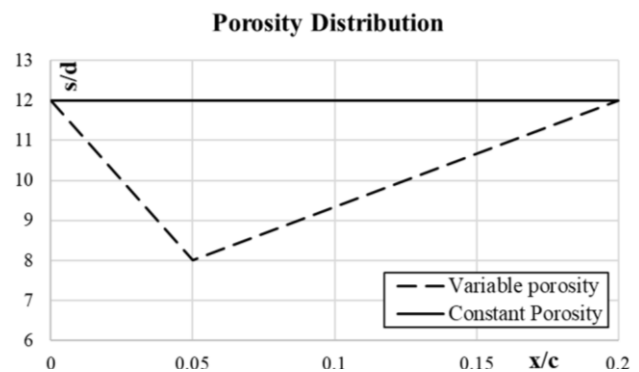


Figure 41 – Hole spacing to diameter ratio distribution for variable and constant porosity panels

In linear stability analysis for transition prediction, there are various approaches in determining the N-factor for transition. For example, in the analysis of the wind tunnel test data carried out in [24], separate values of N-factor for transition onset due to CF and TS instability modes have been

derived, whereas a variation in the N-factor between CF and TS instability modes for transition has been used by various researchers. In the analysis of ARA TWT test data [11] as outlined in Section 6.1, a single value of N-factor of about 7.5 for transition has been determined. There is no universal standard of method for determining the N-factor for transition in linear stability analysis. It depends on how the N-factor is being applied with the transition prediction method and understanding of its behaviour.

In the analysis of ARA TWT data for the HLFC model with a solid panel surface [23], it was found that the N-factor for transition varies with angle of incidence as can be seen in Figure 42, which is contrary to a single N-factor value that was previously assumed [11]. The wave angle at transition location for these cases is shown in Figure 43. Based on the wave angles, transition is due to CF at negative angle of incidence and TS at higher angle of incidence. The results are consistent with the pressure distribution on the upper surface, with a favourable gradient at negative angles of incidence for CF and an adverse gradient at positive angles of incidence for TS, as shown in the pressure distributions presented in Figure 44 for a case at $M=0.7$. It was apparent that the N-factor is particularly lower for conditions corresponding to cases with the presence of both strong CF and TS waves, identified as oblique waves in Figure 42 for cases near zero angle of incidence. The results suggested that the low N-factor may be due to the limitation inherent in the linear methods for cases where there is a possibility of interaction between CF and TS waves. A preliminary investigation using linear and non-linear PSE methods [25, 26] has also been carried out [23]. The non-linear method requires an initial inflow state to seed the simulation, and the initial condition can affect the growth of the instability waves. Although the results have provided support for the most likely instability waves that are responsible for the onset of transition as identified in the linear method, it requires detailed information of the tunnel environmental fluctuation measurements in order to provide a more accurate simulation. Detailed measurement of the tunnel environment and fluctuations within the boundary layer are required in the future.

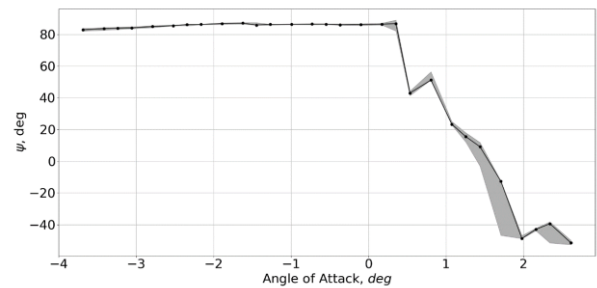
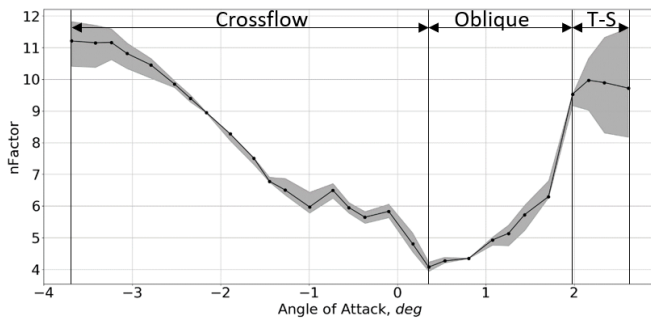
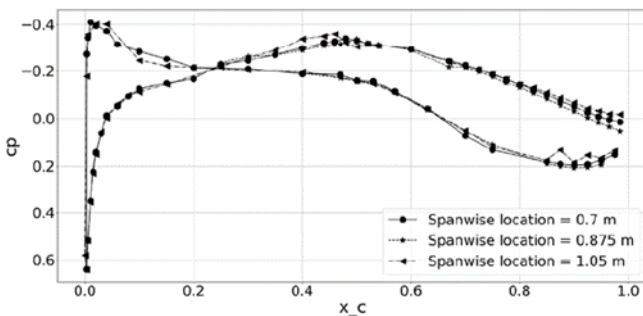
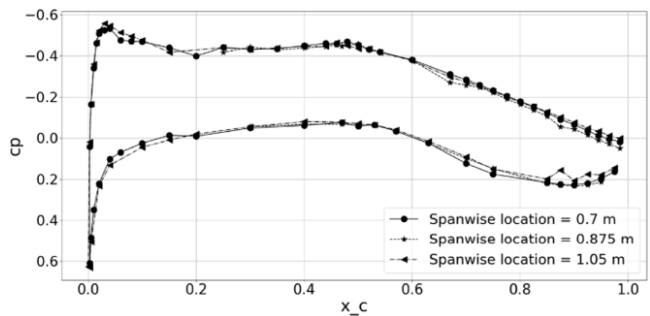


Figure 42 – Transition N-factor correlated with I-R at $M=0.7$

Figure 43 – Wave angle at transition location at $M=0.7$



$\alpha = -1.24^\circ$

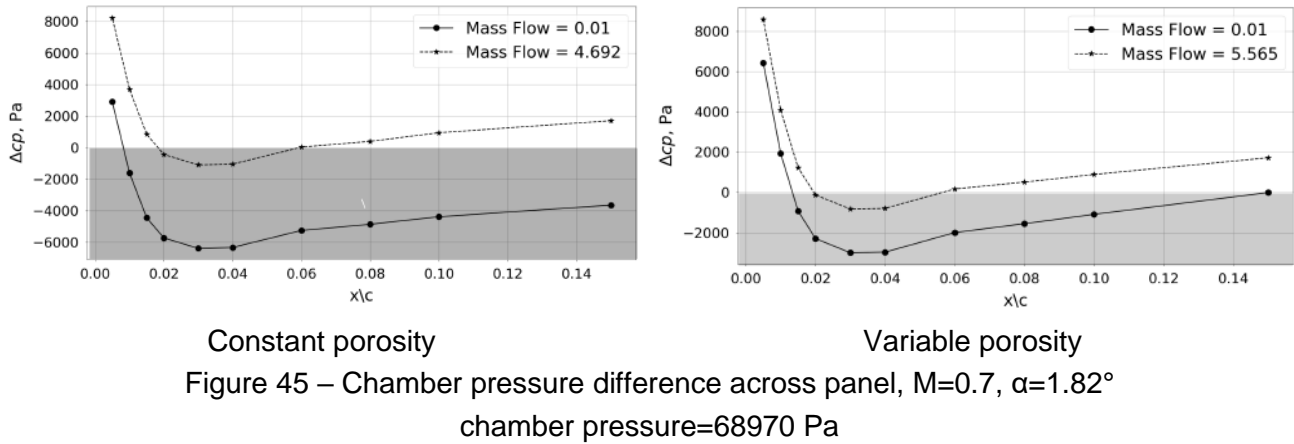


$\alpha = 1.82^\circ$

Figure 44 – Measured pressure distributions at $M=0.7$

For porous panel cases, it was shown that the variable porosity panel has been able to provide a higher suction velocity than the constant porosity panel, as the design has intended. This is illustrated in the results presented in Figure 45 for $M=0.7$ and $\alpha=1.82^\circ$ case with a chamber pressure at 78970 Pa, where the total suction mass flow is higher for variable porosity than constant porosity. It can be seen that for this chamber pressure, blowing is occurring between 2% to 6% chord indicated by the top curve in Figure 45, where the pressure difference across the panel is negative. In HLFC, the

chamber pressure needs to be set low enough to avoid blowing, as blowing can cause transition. For the constant porosity panel, blowing has caused transition within the porous panel region based on IR images recorded in the wind tunnel test. However, for the porous panel case, although blowing was present, the amount of suction achievable downstream of blowing was able to stabilise the flow delaying the onset of transition at 40% chord. This finding is unexpected and should be further investigated in the future, as this would have important implications on the possibility of using surface suction to stabilise the instability due to the effect of surface imperfections on transition.



7. Wind Tunnel Simulation Methodology

Wind tunnel performance testing of aircraft design employing HLFC requires simulation of both the extent of laminar flow and turbulent boundary layer thickness that would occur in flight. For HLFC testing in a cryogenic tunnel, there may be scaling problems associated with the size of the suction holes at model scale at high Reynolds number, and transition is also very sensitive to small surface imperfections where the incorporation of the porous panel for surface suction would be a difficult challenge for model manufacture. For a conventional wind tunnel such as ARA TWT, although conditions at the lower Reynolds number are more favourable for maintaining the extent of laminar flow, there are difficulties in simulating the right turbulent boundary layer thickness at model scale. In addition, since the transition location is already far downstream with HLFC, there is limited margin left for the aft transition fixing technique to simulate the effect of a higher Reynolds number.

A theoretical study to address a number of issues involved in the wind tunnel testing of HLFC wings in a low Reynolds number tunnel and some of the problems related to scale effects has been carried out at ARA [14]. These simulation issues are illustrated by the results shown in Figures 46 and 47 for the same two aerofoils with different types of rooftop pressure distribution as presented in Section 5 of the current paper. With the assumption that the laminar extent at flight scale can be achieved at wind tunnel Reynolds number, there are differences in the pressure distributions, shock positions and drag values between the two Reynolds numbers as would be expected.

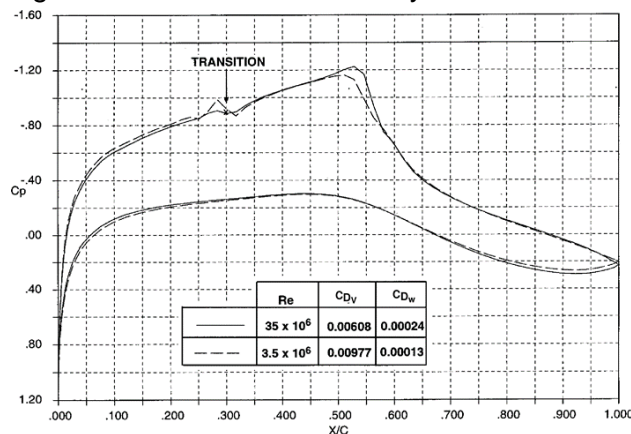


Figure 46 – Effect of Reynolds number, M2303 aerofoil, $M=0.68$, $C_L=0.5$

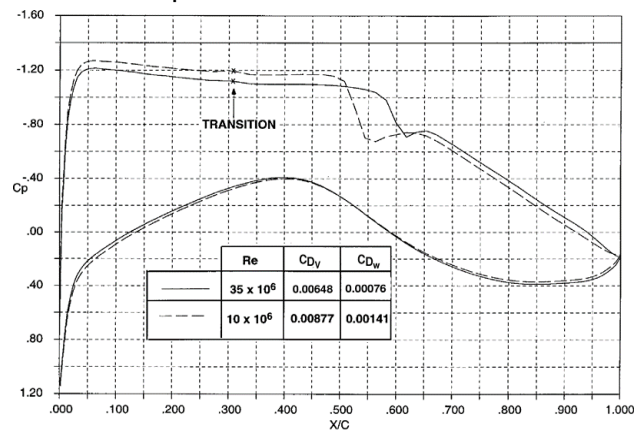


Figure 47 – Effect of Reynolds number, Lock aerofoil, $M=0.72$, $C_L=0.84$

Despite the more favourable conditions for maintaining laminar flow at the lower Reynolds numbers wind tunnel facilities, the extent of laminar flow expected at flight conditions may not be achievable in wind tunnels with a much lower transition N-factor than at flight conditions. In general, the transition location in flight will not be reproduced in the wind tunnel without the use of some method of suppressing the instabilities in order to delay transition. This could be surface suction as in HLFC or surface cooling. The level of cooling required at wind tunnel Reynolds number to stabilize the flow to delay transition to that at flight Reynolds number can be found in Ref [14].

With the assumption that the laminar extent at flight scale can be achieved at wind tunnel scale, the issues of simulating the turbulent boundary layer still need to be addressed. A technique for reducing the turbulent boundary layer thickness in tunnel scale to that of flight scale is the application of suction. It would not be practical to apply surface suction covering the whole of the turbulent flow region, due to the structural constraints of the wind tunnel model. It was found that for the types of pressure distribution and shock positions shown in Figures 46 and 47 for the M2303 and Lock aerofoils, an appropriate location for the application of suction for the reduction of the turbulent boundary layer thickness would be in the region between 65% and 85% chord. The key premise assumed here is that the correct simulation of the boundary layer displacement thickness at the trailing edge will result in a close simulation of the pressure distribution and hence overall aerodynamic performance.

For a pressurised wind tunnel, tunnel pressure can be increased to achieve a higher Reynolds number, known as the Reynolds number sweep test technique. For an atmospheric wind tunnel such as ARA TWT, a number of transition fixed locations aft of the leading-edge can be used to simulate an effective higher Reynolds number, known as the transition sweep technique. With the Reynolds number sweep approach, it would be preferable to keep the level of suction constant as the tunnel Reynolds is increased. Using the M2303 aerofoil as an example, for a case with a suction velocity of -0.004 applied to the upper surface, the effect of increasing Reynolds number on the boundary layer displacement thickness distribution is shown in Figures 48 and 49 for the upper and lower surfaces, respectively. The transition position on the lower surface at tunnel scale for this case is taken at 30% chord instead of 1% chord as in flight, in order to reduce the scale effects on the lower surface. It could be argued that suction could also be applied to the lower surface instead of aft transition fixing. It can be seen that at a tunnel Reynolds number of 12×10^6 , the trailing-edge displacement thickness at tunnel scale has been reduced to that of flight scale. Figure 50 shows that the corresponding pressure distribution and drag values now nearly match the flight scale results. For the Lock aerofoil at 12×10^6 tunnel Reynolds number, a much lower suction velocity ($V_s = -0.0015$) is required to achieve the flight scale results as shown in Figure 51.

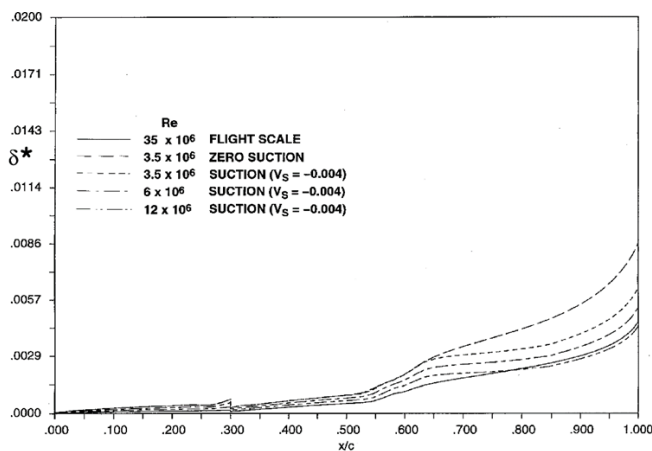


Figure 48 – Upper surface displacement thickness, M2303 aerofoil, $M=0.68$, $C_L=0.5$

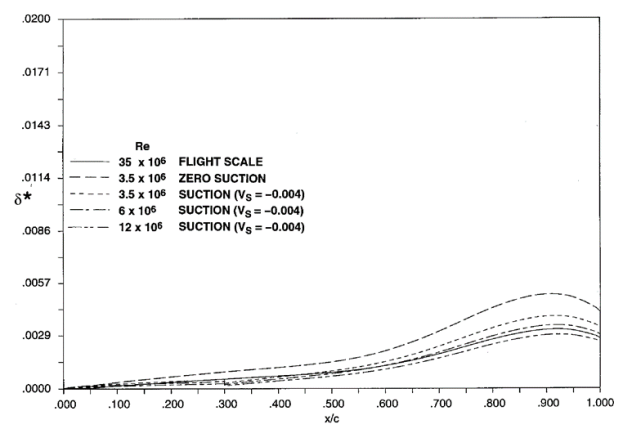


Figure 49 – Lower surface displacement thickness, M2303 aerofoil, $M=0.68$, $C_L=0.5$

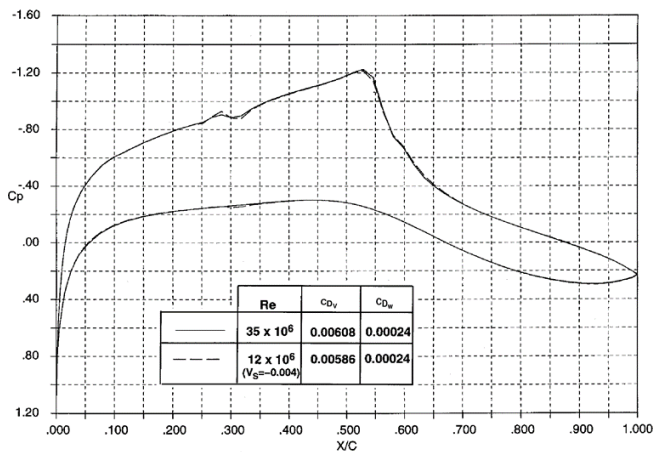


Figure 50 – Comparison of pressure distribution between wind tunnel and flight Reynolds numbers, M2303 aerofoil, $M=0.68$, $C_L=0.5$

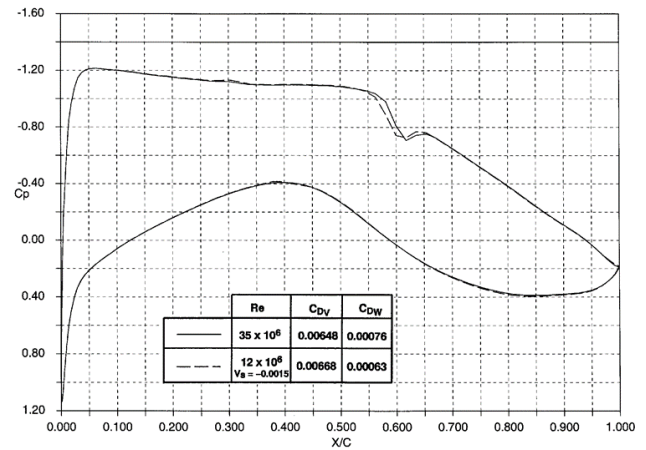


Figure 51 – Comparison of pressure distribution between wind tunnel and flight Reynolds numbers, Lock aerofoil, $M=0.72$, $C_L=0.84$

It was shown that the same suction velocity is applicable across the incidence range, which is of practical benefit for testing. This is illustrated in the results presented in Figures 52 and 53, where the lift and drag performance across the incidence range closely matches that at flight scale Reynolds number. For tunnels with constant Reynolds number, such as the ARA tunnel, where the transition sweep approach would normally be adopted, it may not be possible to fix transition further aft than the flight scale location, since transition is already close to the shock. To simulate the turbulent boundary layer at flight scale, the suction quantities need to be increased. For a chord Reynolds number of 3.5×10^6 , representative of the ARA tunnel, a suction velocity of -0.01 is required to match the flight scale results for the M2303 aerofoil. This is illustrated in the results presented in Figures 54 and 55, where the $C_L \sim \alpha$ and $C_D \sim C_L$ curves at flight scale have also been simulated successfully.

For wings designed with fully turbulent flow, the use of surface suction in the turbulent flow region for flight scale Reynolds number simulation has been demonstrated successfully in an ARA wind tunnel test [27], hence the technique could be used for testing aircraft with HLFC wing design in the future. Further investigation is required to extend the technique to predict buffet onset. The issues involving simulation of the transition zone should also be studied.

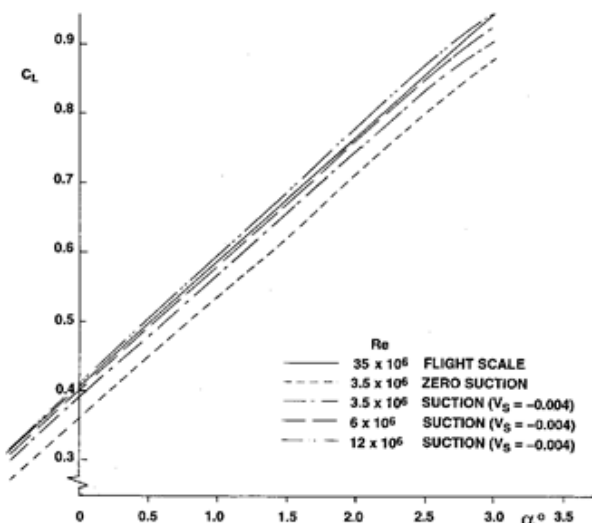


Figure 52 – Variation of C_L with α , Reynolds number sweep technique, M2303 aerofoil, $M=0.68$

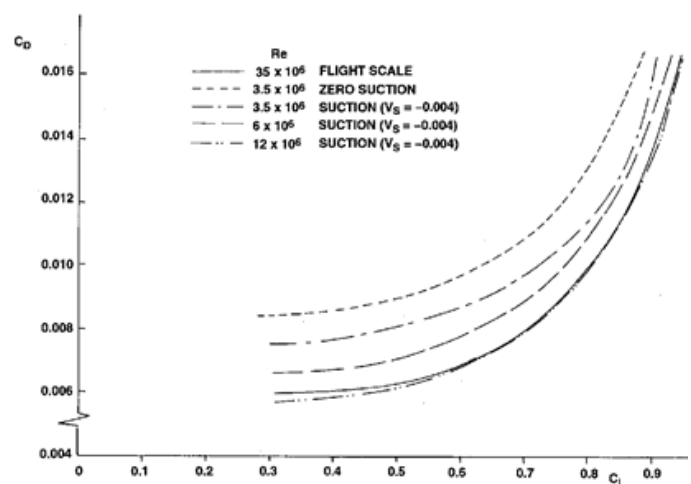


Figure 53 – Variation of C_D with C_L , Reynolds number sweep technique, M2303 aerofoil, $M=0.68$

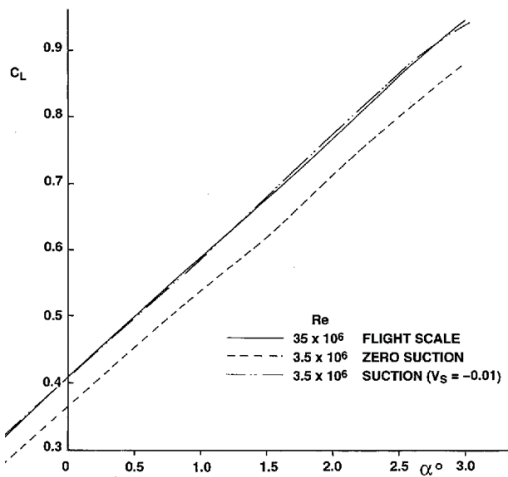


Figure 54 – Variation of C_L with α ,
Transition sweep technique,
M2303 aerofoil, $M=0.68$

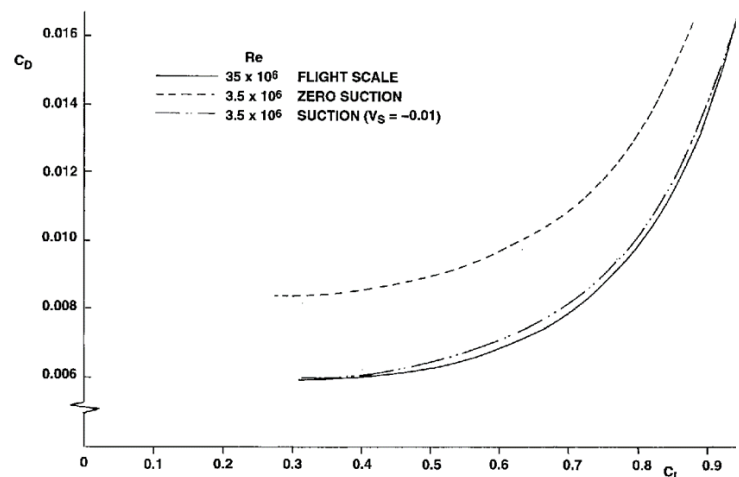


Figure 55 – Variation of C_D with C_L ,
Transition sweep technique,
M2303 aerofoil, $M=0.68$

8. Conclusions and Future Research Recommendations

A methodology of controlling various flow instabilities in order to delay transition for a range of pressure distributions relevant to civil transport aircraft has been established. The structural constraint of requiring the HLFC porous surface to be forward of the wing front spar would limit the extent of laminar flow that can be obtained. Downstream of the front spar, transition is most likely to be caused by TS instability. This constraint may be overcome by the use of surface cooling instead of suction downstream of the front spar for suppressing TS instability in order to achieve a greater extent of laminar flow. The surface cooling rates required for suppressing TS waves are about 10% below the ambient temperature. There is current interest in the use of hydrogen fuel for engine propulsion for zero carbon emissions. Liquid hydrogen storage is among the most promising options, stored in very low temperature in the order of -250°C . The feasibility of using the liquid hydrogen to provide surface cooling to suppress the flow instabilities for delaying transition should be investigated in the future.

The single chamber and variable porosity concept as an alternative HLFC system to the multi-chamber concept has been applied to an Airbus A330 retrofit wing. It was shown that the concept can be incorporated into the wing leading-edge structure with a conventional hot air wing ice protection system and the potential with an electric wing ice protection system. The resulting structural system is less complex and weighs less than the multi-chamber concept. In the future, a more detailed design is required, including structural strength and manufacturing considerations, in order to mature the concept to the aircraft application level. The suction mass flow can be controlled by a combination of hole spacing, hole diameter and skin thickness with the variable porosity concept. The trade-off between the structural stiffness, weight and laser drilling in terms of these parameters for the porous skin should also be investigated.

Aerofoils with different types of 'rooftop' pressure gradients for HLFC application and their aerodynamic performance characteristics have been investigated. Pressure distributions with a favourable 'rooftop' gradient are usually regarded as the most appropriate for maximising laminar flow extent. It should be noted that in addition to viscous drag reduction, wave drag and lift capability are important considerations for HLFC wing design. The design and performance investigation has shown that it is possible to use a turbulent type of pressure distribution for HLFC application for an Airbus A330 retrofit wing, with transition delayed to as far downstream as the shock location. These wing sections have a higher L/D performance and better drag rise characteristics than wing sections with a favourable gradient type of pressure distribution. In the future, more analysis should be carried out to substantiate the aerodynamic performance compared with a conventional aircraft with a turbulent wing design, as this has the potential of being able to retain the performance of a conventional aircraft and implications on aircraft operation, in the case of suction system failure.

The analysis of ARA wind tunnel transition data has shown that it is not possible to use a single critical N-factor for transition prediction with linear stability analysis method. It was found that the N-factor for transition is very low for cases near zero angle of incidence with the presence of strong CF and TS instabilities, where these waves may interact. These cases also coincide with a pressure

distribution relevant to HLFC design. The low N-factor for transition may be due to the limitation of linear stability analysis methods in the case of interaction waves. More work is required to understand this phenomenon with non-linear methods. Detailed measurement of the tunnel environment and fluctuations within the boundary layer are required in the future to enable a more realistic detailed investigation with these methods. The investigation should also be carried out for flight scale Reynolds number, as the choice of N-factor for transition prediction with linear compressible or incompressible stability analysis methods would affect the type of pressure distribution that can be used for HLFC design. This issue needs to be resolved, since choosing a favourable or adverse type of 'rooftop' pressure distribution for HLFC design will have a significant effect on L/D performance and drag rise characteristics.

The effect of the transition region on the aerodynamic performance of HLFC aerofoils have been shown to be significant, indicating that the modelling of the transition region should be included in aerodynamic methods for designing HLFC aerofoils and wings. The full extent of transition from onset to completion has been measured in ARA wind tunnel tests. Analysis of these test data should be extended to transition zone prediction methods in the future.

ARA has acquired wind tunnel testing capability for measuring the effect of small features on transition in NLF, this capability should be extended to HLFC to investigate the effect of suction on the disturbances due to various degree of surface imperfections. For a HLFC wind tunnel test case with variable porosity, it was shown that it may be possible to stabilise the flow even in the presence of blowing with sufficient suction downstream of blowing. The use of the variable porosity concept to provide a higher suction mass flow for controlling the disturbances due to surface imperfections should be investigated.

A theoretical investigation has shown the viability of a wind tunnel testing methodology for HLFC aerofoils using surface suction at wind tunnel Reynolds number to thin the turbulent boundary layer to simulate the viscous flow development at flight scale Reynolds number. The application of this technique has achieved a close simulation of the flight scale results in terms of pressure distributions and aerodynamic forces. This high Reynolds number wind tunnel simulation technique has already been demonstrated in ARA TWT for an aircraft with a fully turbulent flow wing design. The technique should be extended to an aircraft with a HLFC wing design. Further investigation is required to extend the technique to predict buffet onset. The issues involving the simulation of the transition zone should also be studied in the future.

9. Contact Author Email Address

Mailto: peter.wong@ihsmarkit.com

10. Copyright Statement

The authors confirm that they, and/or their company or organization, hold copyright on all of the original material included in this paper. The authors also confirm that they have obtained permission, from the copyright holder of any third party material included in this paper, to publish it as part of their paper. The authors confirm that they give permission, or have obtained permission from the copyright holder of this paper, for the publication and distribution of this paper as part of the ICAS proceedings or as individual off-prints from the proceedings.

References

- [1] Wong P W C and Maina M. An investigation of hybrid laminar flow aerofoil pressure distributions and performance characteristics. *2nd European Forum on Laminar Flow Technology*, Bordeaux, France, June 1996.
- [2] Wong P W C and Maina M. Development and application of methods for laminar flow research at ARA. *ICAS Proceedings*, Sorrento, Italy, ICAS 96-1.7.3, September 1996.
- [3] Wong P W C and Maina M. Study of methods and philosophies for designing hybrid laminar flow wings. *ICAS Proceedings*, Harrogate, UK, ICAS 2000-2.8.2, August 2000.
- [4] Horstmann K, Schrauf G, Sawyers D. and Sturn H A. simplified suction system for a HLFC leading-edge box of a A320 fin. *CEAS Aerospace Aerodynamic Research Conference*, Cambridge, UK, June 2002.
- [5] Wong P W C, Maina M and Doig G C. Drag reduction using boundary layer suction and blowing. *CEAS/Katnet Conference on Key Technologies*, Bremen, Germany, 20 - 22 June, 2005.
- [6] Wong P W C. Laminar flow control and drag reduction for supersonic aircraft configurations. *CEAS/Katnet II Conference on Key Aerodynamic Technologies*, Bremen, Germany, 12 – 14 May 2009.
- [7] Wong P W C and Maina M. An investigation of hybrid laminar flow aerofoil pressure distributions and performance characteristics. *2nd European Forum on Laminar Flow Technology*, Bordeaux, France, June 10-12, 1996
- [8] Wong P W C and Maina M. Development and application of methods for laminar flow research at ARA. ICAS 96-1.7.3, *Proc. of 20th ICAS Congress*, Sorrento, Italy, September 1996.
- [9] Wong P W C and Walters S. Design and performance analysis of a hybrid laminar flow control (HLFC) concept for a civil transport aircraft. *Greener Aviation Conference*, Brussels, Belgium, October 2016.
- [10] Green J E and Wong P W C. Modelling the transition region for laminar flow control applications. *CEAS Aerospace Aerodynamic Research Conference*, Cambridge, UK, June 2002
- [11] Allen N, Lawson S, Maina M and Alderman J. Qualification of the ARA TWT for laminar flow testing. *The Aeronautical Journal*, Vol. 118, Issue 1209, Nov. 2014, pp. 1349-1358.
- [12] Lawson S and Ciarella A. Use of a ring wing model to investigate factors affecting transition measurement using temperature sensitive pint and hot films in transonic flow. *55th AIAA Aerospace Sciences Meeting, AIAA SciTech Forum*, AIAA 2017-1217, 2017.
- [13] Lawson S, Ciarella A and Wong P W C. Development of experimental techniques for hybrid laminar flow control in the ARA transonic wind tunnel. *2018 Applied Aerodynamics Conference*, Atlanta, Georgia, AIAA 2018-3181, 2018.
- [14] Wong P W C and Maina M. Study of wind tunnel simulation methodology for HLFC wings. *Proceedings of CEAS/DragNet European Drag Reduction Conference*, Potsdam, Germany, June 2000.
- [15] Mack L M. Boundary layer linear stability theory. *AGARD Special Course on Stability and transition*, VKI, March 1984.
- [16] Atkin, C. J. Linear stability analysis: Software user manual for CoDS. DERA unpublished.
- [17] Atkin, C.J. Calculation of laminar boundary layers on swept-tapered wings, Part I: Theory. DERA/MSS5/TR980444/1.0, January 2000.
- [18] Cobbin, A.M. Calculation of laminar boundary layers on swept-tapered wings, Part II: Code validation. ARA CR M373/1, January 2000.
- [19] Poll D I A and Paisley D J. On the effect of wing taper and sweep direction on leading-edge transition. *Aeronautical Journal*, March 1985.
- [20] Preist J, and Paluch B. Design specification and inspection of perforated panels for HLFC suction systems. *2nd European forum on laminar flow technology*, Bordeaux, France, 1996.
- [21] Ashill P R, Wood R F and Weeks D J. An improved, semi-inverse version of the viscous Garabedian and Korn method (VGK), RAE TR87002, 1987.
- [22] Narasimha, R. and Dey, J. Transition-zone models for 2-dimensional boundary layers: a review, *Sādhana* November 1989, 14, (2), pp 93-120.
- [23] Ciarella A, Lawson S and Wong P W C. Aerodynamic and transition analysis of the hybrid laminar flow control wing experiment at the ARA wind tunnel. *AIAA Aviation Conference 2019*, 2019-3598, Dallas, 2019.

- [24]Ashill P R, Betts C J and Gaudet I M. A wind tunnel study of transition flows on a swept panel wing at high subsonic speeds. *CEAS 2nd European forum on laminar flow technology*, Bordeaux, June 1996.
- [25]Mughal S M. Stability Analysis of Complex Wing Geometries: Parabolised Stability Equations in Generalised Non-Orthogonal Coordinates. *36th AIAA Fluid Dynamics Conference and Exhibit*, AIAA Paper: 2006-3222, San Francisco, California, 2013.
- [26]Mughal M S. CoPSE/BL-MiPsecR User Manual: A Toolkit for Instability, Receptivity & Transition Analysis, Imperial College, Internal report: Release 3.05.18, 2018.
- [27]Green J E, Elliot M and Wong P W C. High Reynolds number simulation in a transonic wind tunnel by surface suction. *ICAS Proceedings*, Toronto, Canada, ICAS 2002-3.7.1, September 2002.